

Fan Noise Reduction from a Supersonic Inlet

by

William E. Nuckolls, Jr.

Thesis submitted to the Faculty of the
Virginia Polytechnic Institute and State University
in partial fulfillment of the requirements for the degree of

Master of Science

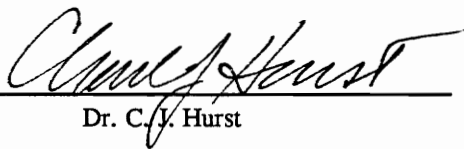
in

Mechanical Engineering

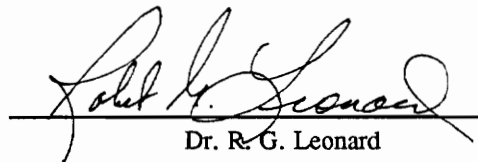
APPROVED:



Dr. W. F. Ng, Chairman



Dr. C. V. Hurst



Dr. R. G. Leonard

January 1992

Blacksburg, Virginia

c.2

5655

V855

1992

N823

C.2

Fan Noise Reduction from a Supersonic Inlet

by

William E. Nuckolls, Jr.

Dr. W. F. Ng, Chairman

Mechanical Engineering

(ABSTRACT)

A series of experiments was conducted to investigate the radiation of fan noise through a supersonic inlet. A scaled-down model of an axisymmetric, mixed-compression, supersonic inlet (P-inlet) was used in conjunction with a 10.4 cm (4.1 in) diameter turbofan engine simulator as the noise source. The tests were conducted at an outdoor facility under static conditions. An attempt is made to reduce the fan noise radiated in the forward sector by modifying the auxiliary inlet doors. The modified doors are designed to reduce the inlet distortion to the fan face. In addition, the new design also uses a converging flow passage in the auxiliary doors in order to take advantage of the noise attenuation due to the choking effect. Both aerodynamic and acoustic measurements are taken in the experiments. The results show that when compared to the original design, the modified auxiliary inlet doors are successful in reducing distortion to the fan face, and that the blade passing frequency tone has been decreased by an average of 6 dB in the forward sector. Results from the closed auxiliary inlet door case are also presented to provide additional comparisons.

Abstract

Acknowledgements

I would like to thank Dr. Wing Ng for his supervision of this research, his guidance has helped me develop as an engineer. I would also like to thank all of Dr. Ng's graduate students who have helped with my research and in making graduate school itself more enjoyable. Special thanks to Zhenguo Yuan and Kevin Detwiler who assisted me with the experiments.

I am grateful for the encouragement received from my family. I would like to thank Bill, my father, and Janet for their financial support when I was an undergraduate. This support allowed me to concentrate on engineering and hence continue my education in graduate school. I also value the words of my mother, Marian, who always reminds me you can do anything if you stay with it and put your mind to it.

Finally, I wish to acknowledge Mary Beth Morris for her friendship and support.

Table of Contents

1.0 Introduction	1
2.0 Previous Research	5
2.1 Differences with Previous Research	8
3.0 The Experiment	9
3.1 Simulator	9
3.2 Supersonic Test Inlets	12
3.3 Aerodynamic Measurements	16
3.3.1 Fan Pressure Ratio	19
3.3.2 Inlet Aerodynamics	22
3.4 Acoustic Measurements	22

4.0 Results	30
4.1 Aerodynamic Results	30
4.1.1 Matching Operating Conditions	30
4.1.2 Inlet Distortion	32
4.1.3 Inlet Aerodynamic Performance	43
4.2 Acoustic Results	46
4.2.1 Sample Spectrum Data	46
4.2.2 BPF Tone versus Angle	49
4.2.3 Comparison with Previous Research	52
5.0 Conclusions and Recommendations	56
5.1 Conclusions	56
5.2 Recommendations	58
Appendix A. Centerbody Effect	61
References	66
Vita	68

List of Illustrations

Figure 1. Supersonic Inlet Features	7
Figure 2. Turbofan Engine Simulator	11
Figure 3. Baseline Supersonic Inlet (P-inlet)	13
Figure 4. Baseline vs. Modified Auxiliary Doors	14
Figure 5. Baseline vs. Modified Inlet	15
Figure 6. Inlet Assembly Drawing	17
Figure 7. Simulator and Modified Inlet	18
Figure 8. Fan Kiel Probe Locations	20
Figure 9. Pitot-Static Probe Locations	23
Figure 10. Pitot-Static and Kiel Probe	25
Figure 11. Measurement Equipment	27
Figure 12. Microphone Layout	28
Figure 13. Hypothetical Mach Number Contours at Fan Face	33
Figure 14. Inlet Mach Number Distribution at Fan Face	35
Figure 15. Closed Door Mach Number Distribution at Fan Face	37

Figure 16. Inlet Mass Flow Distribution	39
Figure 17. Inlet Fan Face Total Pressure Recovery (%)	41
Figure 18. Fan Pressure Ratio Distribution at Fan Exit	42
Figure 19. Inlet Mach Numbers	44
Figure 20. Inlet Total Pressure Recovery (%)	45
Figure 21. Sample Data (Baseline vs. Modified)	47
Figure 22. Sample Data (Baseline vs. Closed)	48
Figure 23. BPF Tone vs. Angle (Baseline vs. Modified)	50
Figure 24. BPF Tone vs. Angle (Baseline vs. Closed)	51
Figure 25. Polar Plot of BPF Tone	53
Figure 26. Delta BPF Tone (Baseline minus Closed)	54
Figure 27. Centerbody Effect on the Mach Number	62
Figure 28. Choking Effect on the Broadband Noise	63
Figure 29. Choking Effect on the BPF Tone	64

List of Tables

Table 1. Kiel Probe Coordinates	21
Table 2. Pitot-Static Probe Coordinates	24
Table 3. Average Fan Pressure Ratio	31
Table 4. Mach Number Distortion in the Circumferential Direction	38
Table 5. Reynolds Number Comparison	57

Nomenclature

BPF	blade passing frequency
CFD	computational fluid dynamics
dB	decibel, sound pressure level, reference pressure 20×10^{-6} pascals
Hz	hertz, frequency
M	Mach number
R_1	distance between inlet centerline and cowl lip
rpm	revolutions per minute
x/R_1	normalized axial position

1.0 Introduction

There is an increase in the need for a supersonic transport as more people travel longer distances. A supersonic aircraft can reduce the flight time significantly on long distance flights, which is important to many people and businesses that now have divisions throughout the world.

For a supersonic transport to be successful, its environmental impact must be minimized. Environmental issues are an increasingly important part of most large engineering projects. With a supersonic transport, the issues involve upper atmosphere emissions, airport community noise, and the sonic boom. All of these topics are currently being researched to determine their potential effect on the environment.

To better understand the impact of a supersonic transport on airport community noise, an experimental test program has been conducted. The program focuses on turbomachinery noise and in particular fan noise radiation through a supersonic inlet. Even though jet noise is the predominant noise source, previous analyses "indicate that forward-propagated fan noise is a significant component during take off and approach," from reference 1. Supersonic inlets are complex and include many variable features for

aerodynamics reasons. The acoustic effect of these variable features on the noise generating mechanisms involved is not yet fully understood.

The motivation of the test program is to reduce the turbomachinery noise radiating forward from a supersonic inlet. This involves understanding the noise mechanisms and how they are affected by the various inlet features. The program involves the testing of a small-scale supersonic inlet connected to a 10.4 cm (4.1 in) diameter turbofan engine simulator. Another motivation of the test program is to demonstrate that a small scale 10.4 cm (4.1 in) diameter simulator can be used as a tool for preliminary acoustic testing. To this end, results from the 10.4 cm (4.1 in) diameter simulator will be compared to previous results obtained at NASA Lewis Research Center, from a test program using a larger 50.8 cm (20 in) diameter simulator, as discussed in reference 2. The reason for using the 10.4 cm (4.1 in) simulator is to reduce the cost of an experiment. The 10.4 cm (4.1 in) simulator can be used as an initial source of experimentation to test multiple concepts. Money and time can be saved by giving initial results and pointers to trends before a design is tested in a more expensive, large-scale test program. Because of the number of variable geometric features associated with the inlet, the experimental test matrix can be large. The 10.4 cm (4.1 in) diameter simulator can be used to simplify these large test programs.

Specifically, the objective of this research is to reduce forward propagating fan noise by modifying the auxiliary door geometry. Supersonic inlets are designed with a small inlet capture area for optimum cruise performance. However, the inlet capture area at cruise conditions is too small for low speed flight. The auxiliary doors are therefore

needed to provide additional air to the engine during takeoff and landing. The auxiliary doors must be opened during low flight speed.

The auxiliary inlet door geometry is modified to include two noise attenuating features. The first goal is to decrease the distortion at the fan face. This goal is accomplished by modifying the auxiliary door to provide a more uniform air distribution to the engine. It will be shown that this modification produces a more steady blade loading, and will therefore reduce fan noise. Decreased inlet distortion is also important for aerodynamic reasons, it allows the engine to operate with a greater stall margin. Second, the doors have been modified to employ the "choking effect." The "choking effect" is the term given to a high Mach number flow which attenuates radiated noise. As a sound wave travels out of an inlet, it must propagate through the incoming air flow. When the incoming air flow in an inlet increases, the amount of time for a sound wave to propagate forward also increases. This increase in time allows more of the sound wave to be dissipated while propagating out of the inlet. This dissipation reduces the radiated noise, thereby employing the "choking effect." This overall objective to reduce noise by modifying the auxiliary door is unique because there is no known previous research with this goal.

In addition to the original and modified auxiliary door configurations, a closed door case is presented. The closed door case is used to provide an initial reference and a comparison with some of the previous research. Altogether, the program involves three supersonic inlet configurations: original, modified, and closed auxiliary inlet doors. Aerodynamic tests are conducted to assist in the understanding of the acoustic results.

The thesis is organized into five separate chapters. Chapter 2 presents the previous research involving supersonic inlets. Chapter 3 explains the experimental setup and procedures of the test program as well as the detailed auxiliary inlet door geometry modifications. The different aerodynamic measurements and their locations are shown. Chapter 3 also explains the acoustic measurements and shows the different microphone positions. The results from the aerodynamic and acoustic test program are explained in Chapter 4. Chapter 5 highlights the conclusions and also makes recommendations for further testing.

2.0 Previous Research

Most of the research with supersonic inlets has taken place under the Supersonic Cruise Aircraft Research program. Most of the previous work is related to the aerodynamic performance of a supersonic inlet, detailed in references 1 and 3 through 7. References 2 and 8 pertain to acoustic test programs. Reference 2 is the only known work to present the acoustic effects of open versus closed auxiliary inlet doors. References 9 and 10 report full scale inlet acoustic testing conducted on the YF-12 aircraft which led to the SR-71 Blackbird.

Under the Supersonic Cruise Aircraft Research program, NASA Lewis initiated a program to experimentally determine the aerodynamic and acoustic performance of a representative supersonic cruise inlet. A 1/3 scale model of an axisymmetric mixed-compression supersonic inlet, named the "P-inlet," was chosen as the testbed for the experiments. The name P-inlet does not refer to any special feature, it is just a name designated for the supersonic inlet. The P-inlet has a 24.86 cm (9.788 in) radius at the cowl lip and is designed for Mach 2.65 cruise. Reference 1 gives the coordinates for the geometry of the P-inlet. The fluid properties of supersonic flow dictate that a supersonic

inlet must have a variety of complex features. These features are shown in Figure 1 and include: a translating centerbody, a boundary layer bleed system, and auxiliary inlet doors. The P-inlet incorporates all of these variable features. The inlet was coupled to a 0.4066 scale JT8D fan simulator, which was powered by an air turbine. The simulator had a 50.8 cm (20 in) diameter fan that was connected to the inlet exit. The P-inlet is designed to deliver air to the fan face at Mach 0.6. The NASA Lewis research was primarily conducted in their 9x15 foot anechoic wind tunnel.

The previous acoustic research programs concentrated on the far-field noise propagation of both the fan fundamental Blade Passing Frequency (BPF) tone and broadband noise. The research focused on changing the centerbody position, bleed system, and auxiliary door configuration to determine their influence on the noise. One of the main findings was that opening the auxiliary doors significantly increases the fundamental BPF tone. The increase in tone was suspected to be caused by the auxiliary doors increasing the flow distortion to the fan. The previous research has also pointed out other noise mechanisms. The current need is to better understand these noise mechanisms to develop better methods to decrease the noise. The research presented in this thesis in general follows the previous research, by investigating the fan noise propagation, but also presented is the new research involving the modification of the auxiliary door to reduce noise.

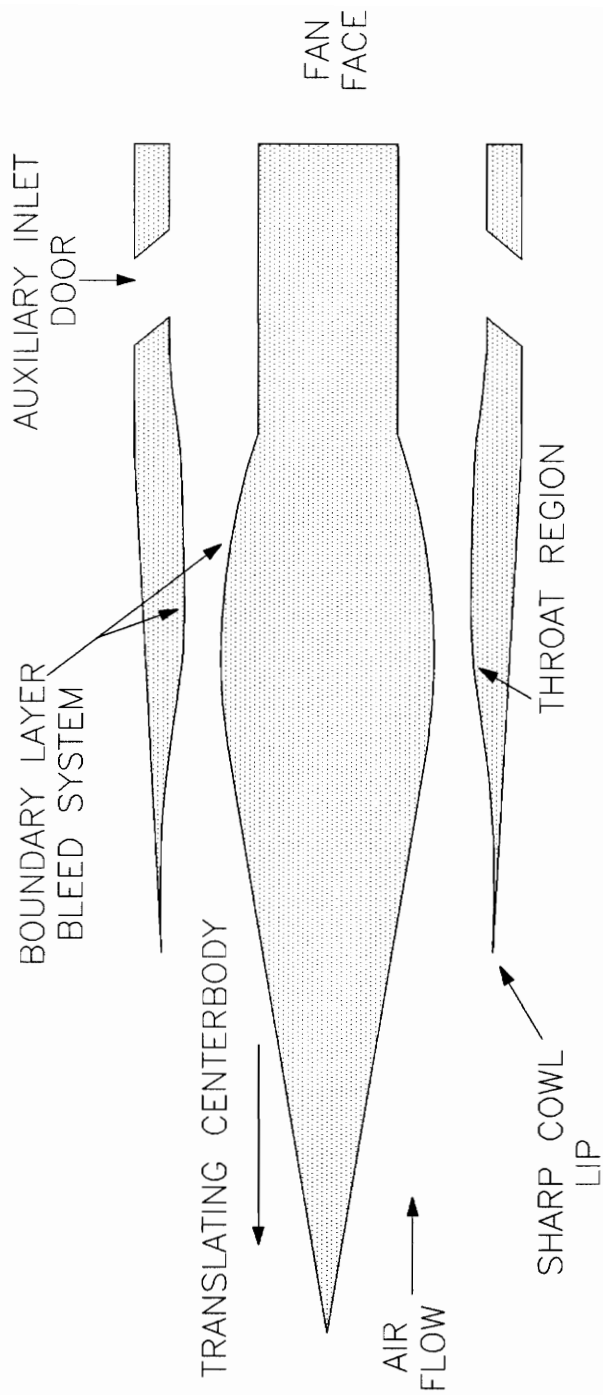


Figure 1. Supersonic Inlet Features

2.1 Differences with previous research

Most of the variable features of the P-inlet, with the exception of the boundary layer bleed system, have been used in the small-scale inlet. The boundary layer bleed system is used to prevent shock-boundary layer separation at cruise conditions and to provide stability to the shock system. At low flight speed conditions the bleed system actually works in reverse by providing airflow from outside to inside the inlet. This flow reversal is a problem because it adds to the inlet distortion and turbulence. In previous testing, the bleed system itself created a noise source. Also, to construct a bleed system for the present small-scale inlet would be complicated. For these reasons, a bleed system was not incorporated into the test inlet. With the exception of the bleed system, all the other variable features of the P-inlet have been incorporated into the small-scale inlet.

3.0 The Experiment

This chapter is divided into four sections. The first section describes the simulator and its operating conditions. Second, the different auxiliary inlet door geometries will be presented. This section will discuss modifications made to the auxiliary door geometry in order to reduce the noise radiation. The third and fourth section will elaborate on the aerodynamic and acoustic measurements respectively.

3.1 Simulator

The turbofan engine simulator provides the airflow in the inlet and is also the noise source. The simulator is a Tech Development Inc., Model 460. The Model 460 has been used previously to simulate the Pratt and Whitney JT9D engine in aerodynamic test programs. Also, a variation of the Model 460 has been used by Pratt and Whitney, in references 11 and 12, to perform acoustic research. The design speed of the Model 460 simulator is 80,000 rpm. The turbofan simulator has a 10.4 cm (4.1 in) diameter fan

with 18 blades and 26 stators. The fundamental BPF tone is "cut-on" because of the low number of stators. The "cut-on" versus "cut-off" theory was developed by Tyler and Sofrin, reference 13. The theory shows that by choosing the proper number of rotor versus stator blades, the rotor-stator interaction noise can be designed to propagate or decay rapidly within the inlet. If there are at least twice the number of stator blades as rotor blades, then the fundamental BPF tone will be "cut-off." "Cut-off" implies that the fundamental BPF tone caused by rotor-stator interaction noise will decay rapidly within the inlet.

Figure 2 shows the turbofan engine simulator, at the top of the figure is the engine casing. At the bottom of Figure 2 is the rotating assembly with the fan on the left and turbine on the right. This assembly fits into the engine casing. Compressed air, stored in tanks, is expanded through the turbine to power the simulator. The turbine power is transferred, by a shaft, directly to the fan. The wires are for the speed pickup and monitoring the temperature of the simulator's bearings.

In the experiment, the simulator was tested at 50,000 rpm (58% design speed), for all of the test cases. At this speed, the simulator generates noise in the pure tone spectrum. The reason for testing at this speed is because the pure tone noise is expected to be a significant noise source during the aircraft landing approach. At this speed the BPF is at 15,000 Hz, with a blade tip Mach number of 0.77. The relative Mach number in the rotating reference frame of the blade is higher than the tip Mach number, but still less than sonic, so the noise is in the pure tone spectrum. The pure tone noise spectrum is characterized by a sharp increase in the noise at the BPF. If the blade tip Mach

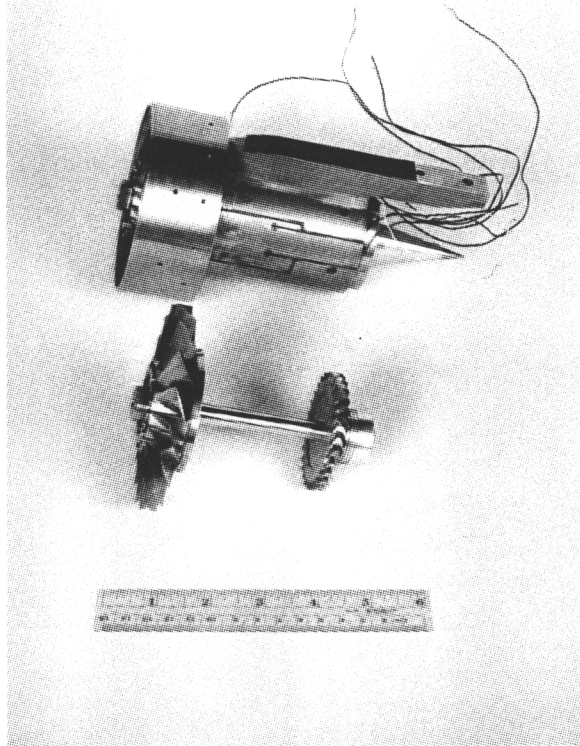


Figure 2. Turboman Engine Simulator

number of the fan was greater than one, then the noise generated would change to the multiple pure tone noise spectrum. The multiple pure tone noise is characterized by many tones throughout the spectrum, caused by the shock waves formed at the fan blades.

3.2 Supersonic Test Inlets

A small-scale model of the P-inlet was designed and constructed for testing. The small-scale model of the P-inlet is referred to as the baseline inlet. The baseline inlet features the same auxiliary inlet door geometry as the P-inlet. Figure 3 shows a side and back view of the baseline inlet. The main feature to note is the position of the auxiliary inlet doors. There are four doors equally spaced, each spanning 50° . In the back view the four struts supporting the centerbody are shown, also equally spaced. The baseline inlet is tested and the results are compared to those obtained from the modified auxiliary door design.

Figure 4 is a side view of the two different auxiliary door designs. At the top is the baseline and at the bottom is the modified door design. The important aspect of the modified door is the converging flow area. This modification is an attempt to employ the choking effect in the auxiliary door. The baseline and modified doors both have the same "exposed" area on the outside of the inlet. Figure 5 is a comparison of the two inlets and demonstrates that the modified design spans a greater percentage of the circumference. The modified inlet has four equally spaced auxiliary doors. Each modified auxiliary inlet

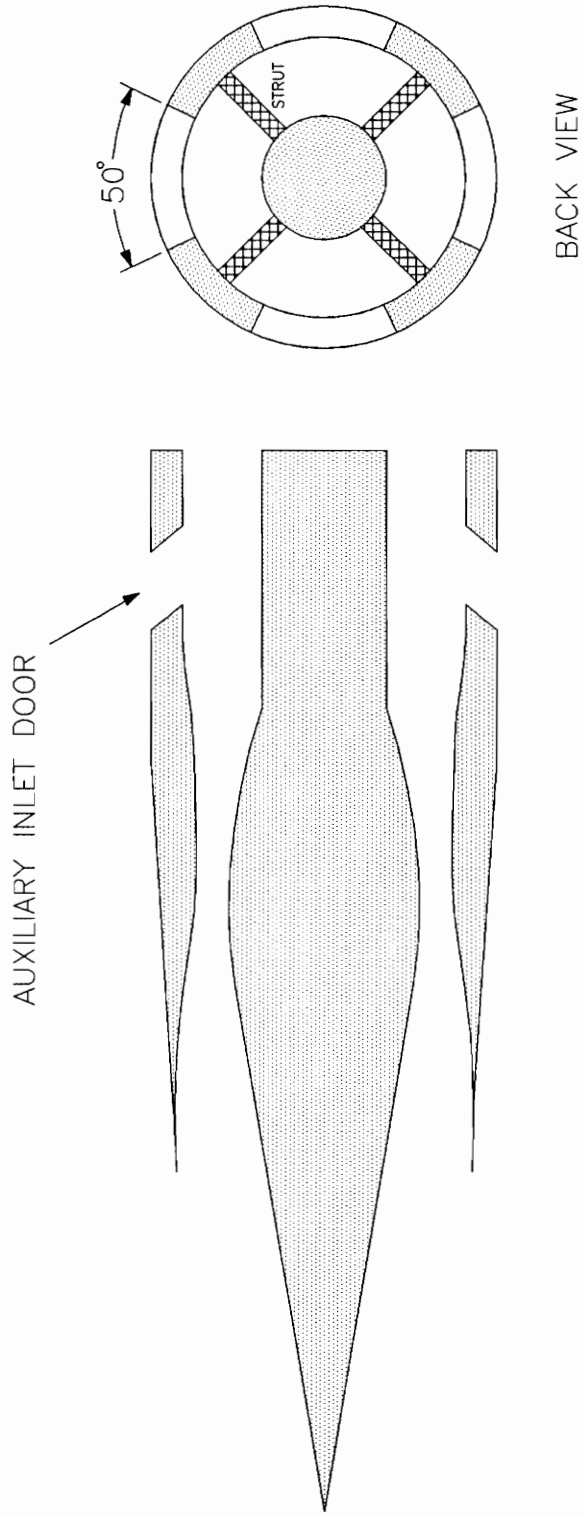


Figure 3. Baseline Supersonic Inlet (P-inlet)

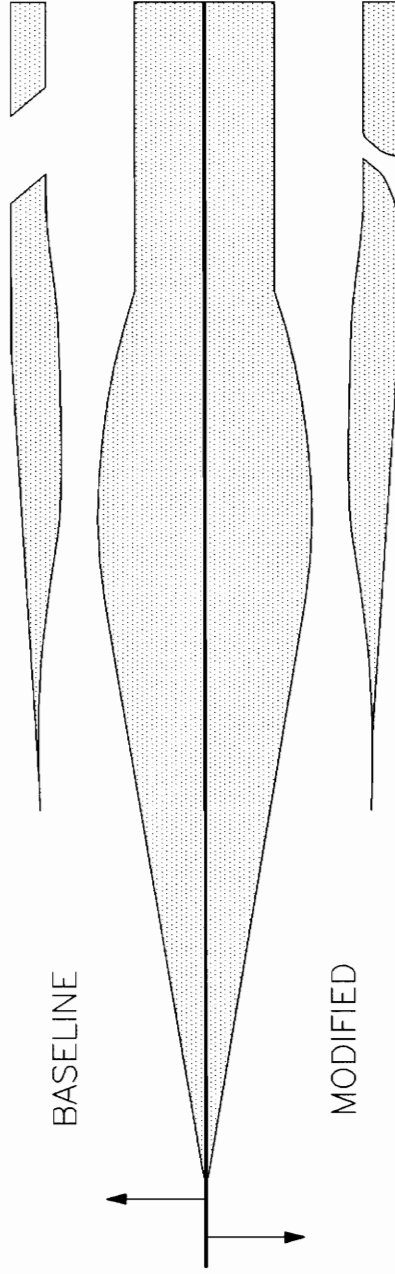
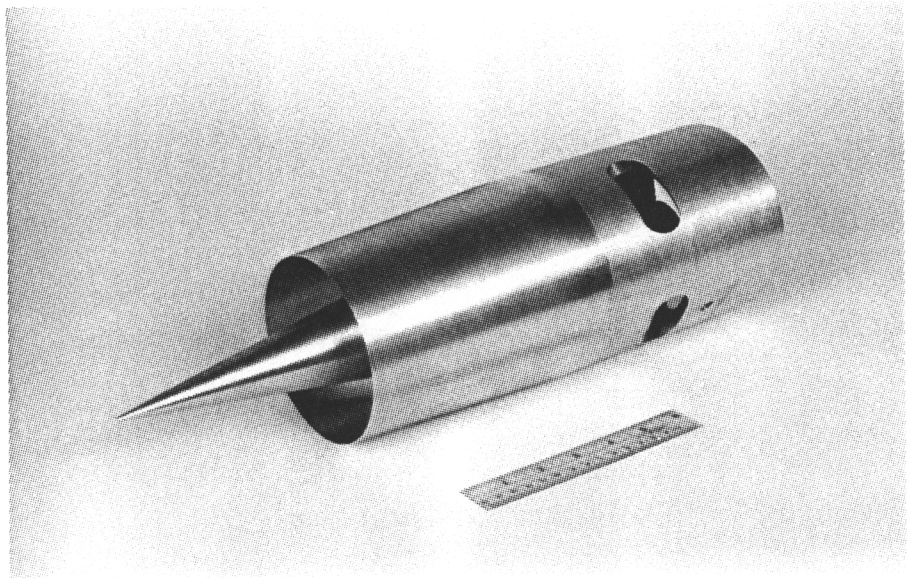
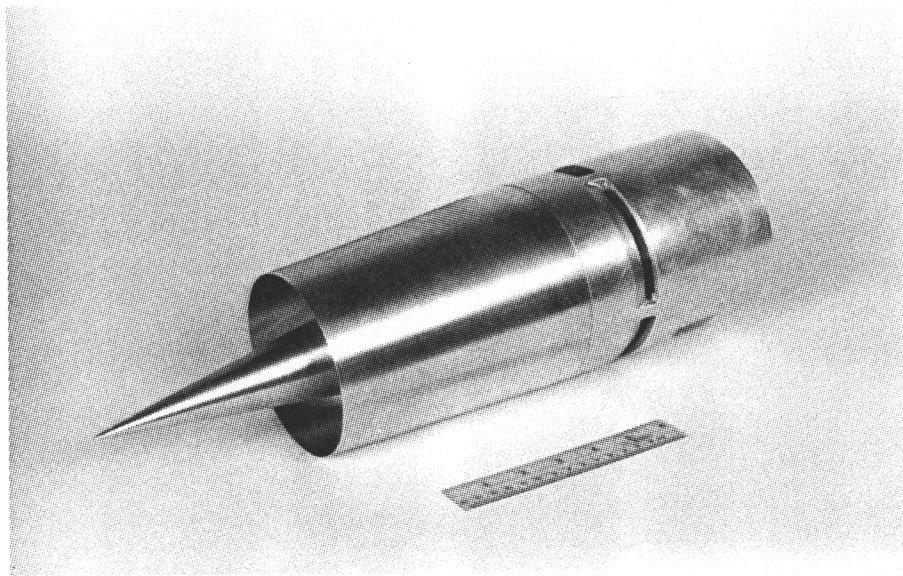


Figure 4. Baseline vs. Modified Auxiliary Doors



Baseline



Modified

Figure 5. Baseline vs. Modified Inlet

door spans 83° in an attempt to have the auxiliary door provide a more uniform air distribution to the fan face.

Figure 6 is a complete assembly drawing of the test inlet. This drawing shows the strut locations and the cross-section of a strut. The purpose of the four struts is to hold the centerbody in the inlet. The test inlet has an overall diameter of 12.7 cm (5 in) and length of 43.7 cm (17.2 in). Figure 7 shows a back view of the simulator and modified inlet connected. The closed auxiliary inlet door case is accomplished by positioning a ring on the inlet. The ring slides on the outside of the inlet and completely covers the auxiliary inlet doors.

3.3 Aerodynamic Measurements

Aerodynamic measurements are needed for two reasons. First, the aerodynamic measurements are used to match the fan's operating conditions when comparing the baseline and modified inlet. This comparison insures that a difference in noise cannot be attributed to a difference in fan pressure ratio or mass flow rate. Since the simulator's rpm is constant for all of the test cases, only the fan mass flow or pressure ratio is needed to match the fan's operating condition. The fan pressure ratio was chosen to determine the fan's operating condition. Second, the aerodynamic measurements are used to determine the inlet performance. The objective is to understand the influence of the aerodynamics on the acoustics. Two aerodynamic measurements were taken at all of the

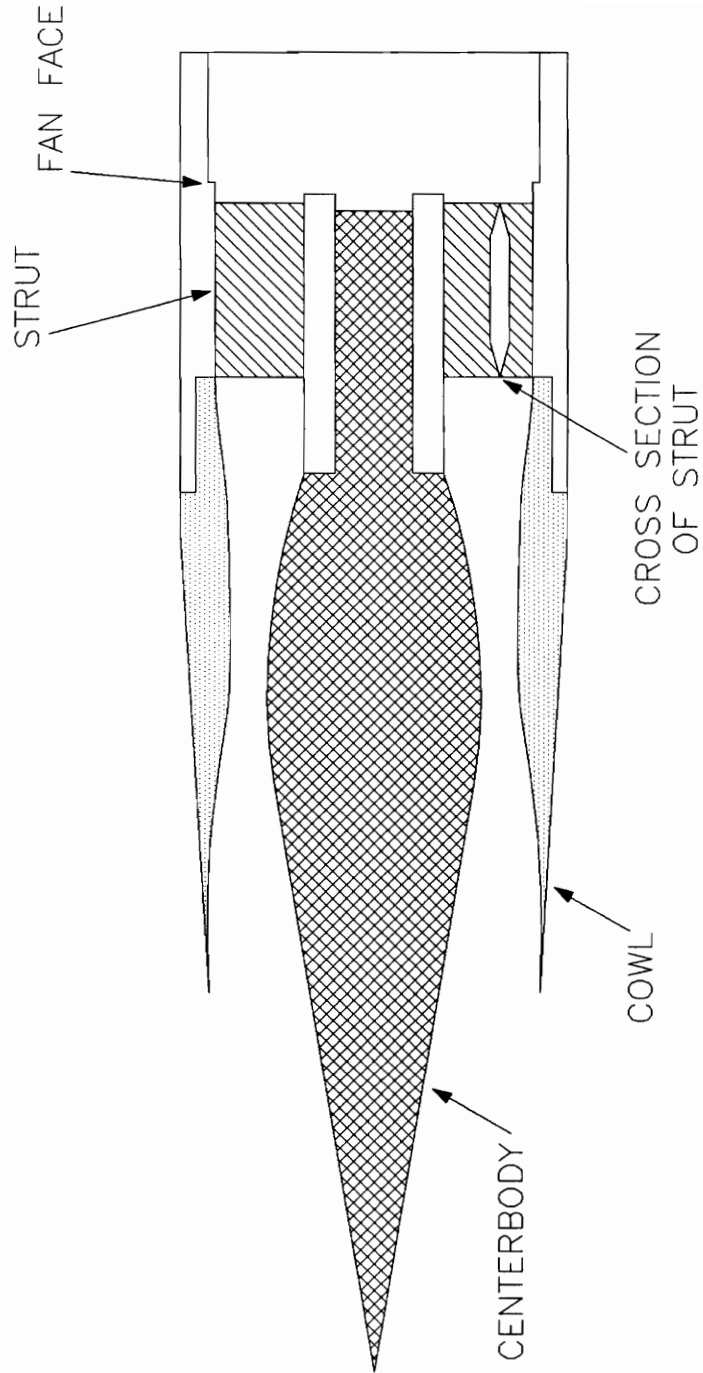


Figure 6. Inlet Assembly drawing

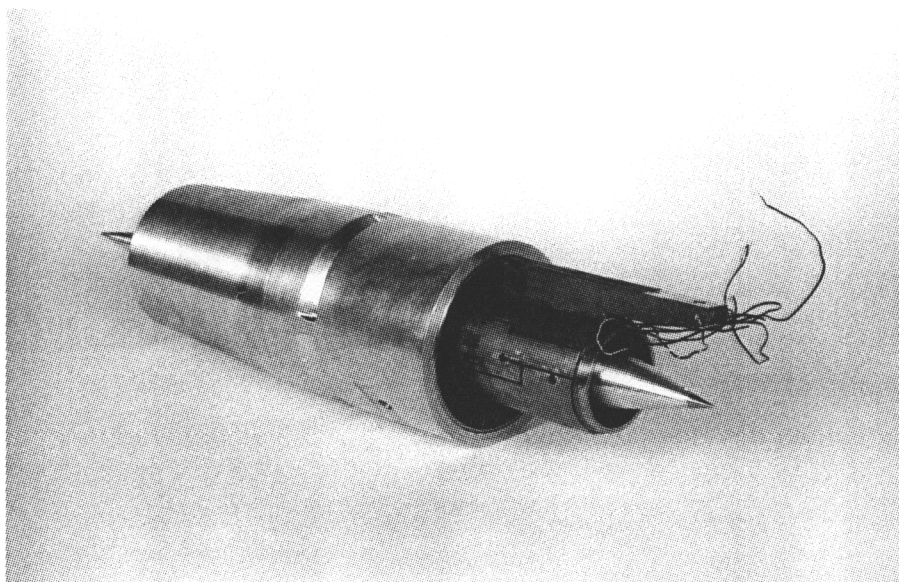


Figure 7. Simulator and Modified Inlet

different probe locations, and the measurements were repeatable.

3.3.1 Fan Pressure Ratio

A Kiel probe was chosen to measure the fan pressure ratio because it is insensitive to flow angularity. The probe was connected to a mercury manometer. The Kiel probe measurement locations are shown in Figure 8. At the top is a side view of the fan and stator assembly showing the probe's three radial positions, both in front of and behind the fan. At the fan exit, the probe was placed in five different circumferential locations ($0^\circ, 22.5^\circ, 45^\circ, 67.5^\circ, 90^\circ$). In the front of the fan, due to symmetry, it is only necessary to place the probe at three different circumferential locations ($0^\circ, 22.5^\circ, 45^\circ$). Table 1 lists the Kiel probe coordinates. The coordinates are normalized with respect to inlet radius (R_i), which is the distance between the inlet centerline and the cowl lip. The axial location at the tip of the centerbody (x/R_i) is designated as zero. The fan pressure ratio is calculated by dividing the fan exit total pressure by the fan entrance total pressure, at the same corresponding radius. The individual results are then area averaged to determine the overall fan pressure ratio.

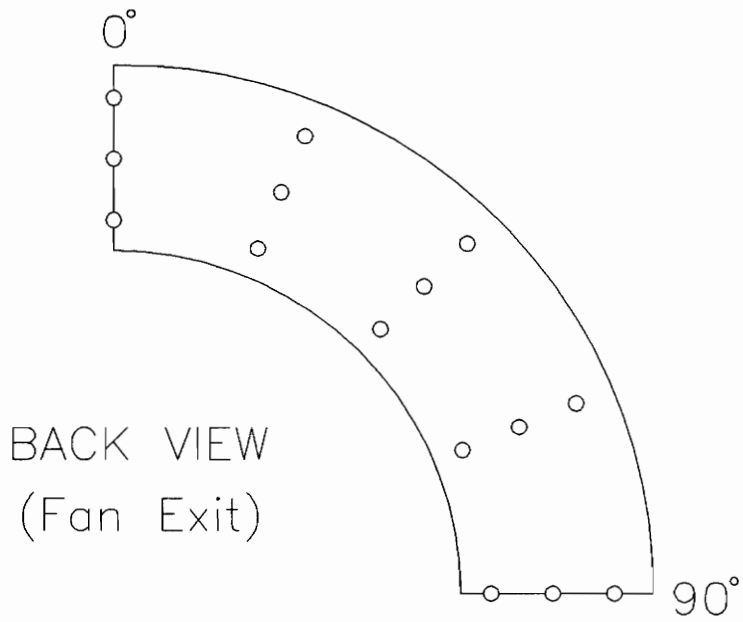
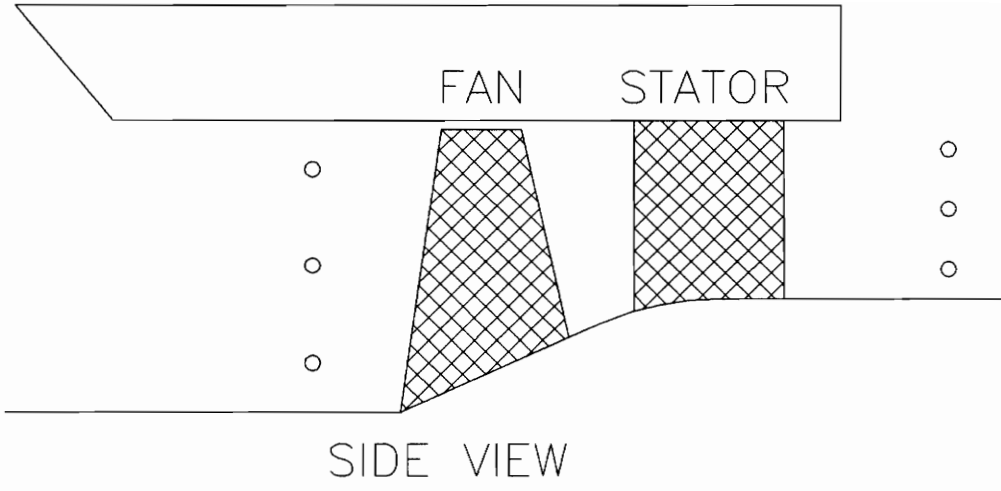


Figure 8. Fan Kiel Probe Locations

Table 1. Kiel Probe Coordinates

$R_1 = 5.43 \text{ cm}$ (2.138 in)	Fan Entrance $x/R_1 = 7.103$	Fan Exit $x/R_1 = 8.259$
Outside r/R_1	0.869	0.906
Middle r/R_1	0.690	0.794
Inside r/R_1	0.511	0.683

3.3.2 Inlet Aerodynamics

A pitot-static probe was used to determine the inlet performance. The pitot-static probe provides measurements of both the Mach number and total pressure recovery of the inlet. The pitot-static probe was placed in the inlet at three axial stations, as seen in Figure 9. At each station, measurements were taken at three radial locations. Additional measurements were taken at the fan station with three circumferential angles ($0^\circ, 22.5^\circ, 45^\circ$). At the fan station, in order to place the probe in the inlet at 0° , one of the struts had to be removed. The three circumferential measurements are needed to establish the effect of the different auxiliary doors on the flow field entering the fan. The probe was positioned as close as possible to the fan face. Additional circumferential measurements were taken at the lip and throat station. The results verified that there are no circumferential variations at the lip and throat station, so these results will not be presented. Table 2 lists the pitot-static probe coordinates. Figure 10 displays the 1.6 mm (1/16 in) pitot-static and the 1.6 mm (1/16 in) Kiel probe.

3.4 Acoustic Measurements

The acoustic measurements were conducted at an outdoor facility. Preliminary testing was performed in an anechoic chamber, however the chamber had an inadequate air supply. The tests were "static" meaning air was pulled into the inlet from the ambient

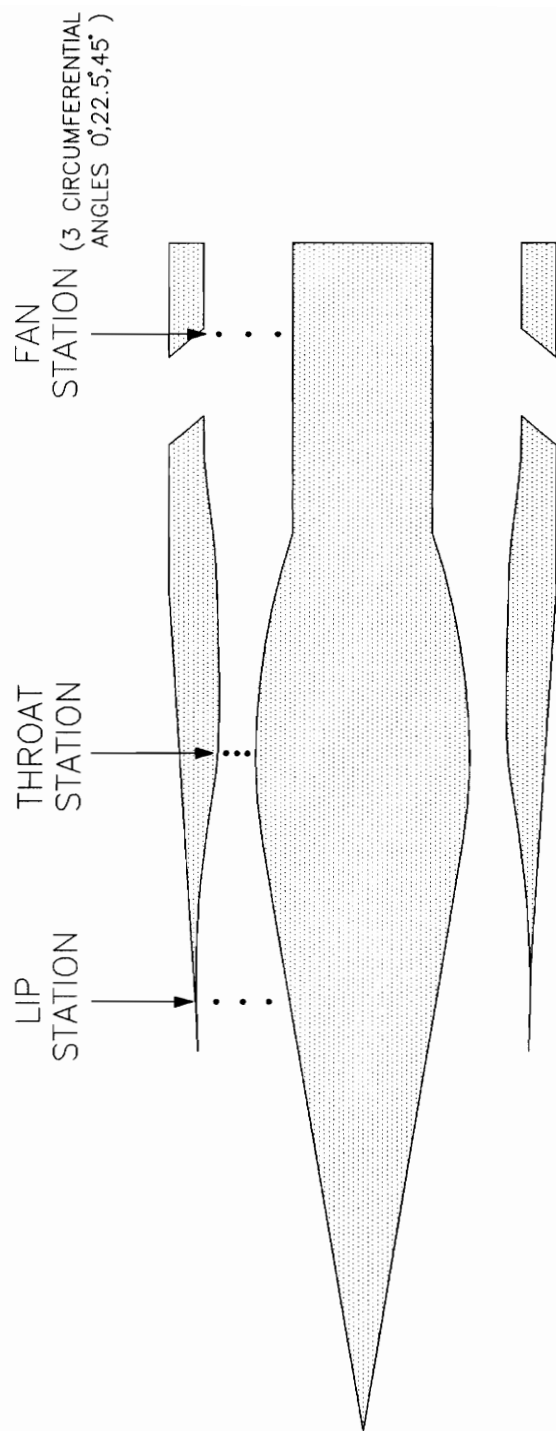


Figure 9. Pitot-Static Probe Locations

Table 2. Pitot-Static Probe Coordinates

$R_1 = 5.43 \text{ cm}$ (2.138 in)	Lip Station $x/R_1 = 2.630$	Throat Station $x/R_1 = 4.150$	Fan Station $x/R_1 = 6.708$
Outside r/R_1	0.853	0.817	0.869
Middle r/R_1	0.712	0.760	0.690
Inside r/R_1	0.561	0.703	0.511

Pitot-Static

Kiel

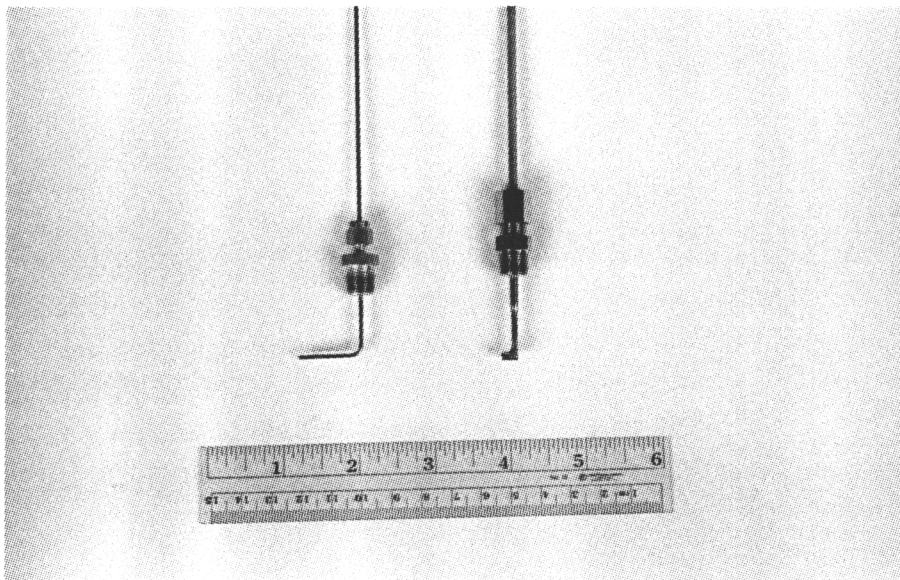


Figure 10. Pitot-Static and Kiel Probe

surrounding atmosphere. Static testing can introduce various instabilities into the measurements. For instance, a ground vortex can be formed and pulled into the inlet. Also, the affect of atmospheric turbulence can be intensified when conducting static tests. These factors tend to increase the unsteadiness in acoustic measurements. To minimize these factors and to help simulate actual flight conditions, inlet control devices have been used to cover subsonic inlets in previous research. An inlet control device has not been included on the supersonic inlet because an inlet control device will not cover the auxiliary inlet doors. In order to decrease the effect of the various instabilities, ten measurements were taken at each microphone position.

The instrumentation used to collect the acoustic data was a Bruel & Kjaer dual channel signal analyzer type 2034. The Bruel & Kjaer analyzer was configured to measure a narrow band spectrum using a Hanning window with 50% overlap. The analyzer was configured to make 3 linear averages with each measurement at a maximum frequency range of 25.6 kHz. More linear averages were preferred, but the air supply limited the duration of the run time. Also used were Bruel & Kjaer condenser microphones type 4136. A personal computer was used to record the acoustic data into permanent memory storage. A digital counter was used to monitor the simulator rpm, while a digital thermometer was used to monitor the bearing temperatures in the simulator. Figure 11 shows some of the aforementioned measurement equipment.

To minimize the effect due to a ground vortex, the simulator was placed 117 cm (46 in) above the ground on a test stand. The microphones were positioned at the same height above ground and centered about the inlet cowl lip, as shown in Figure 12. The

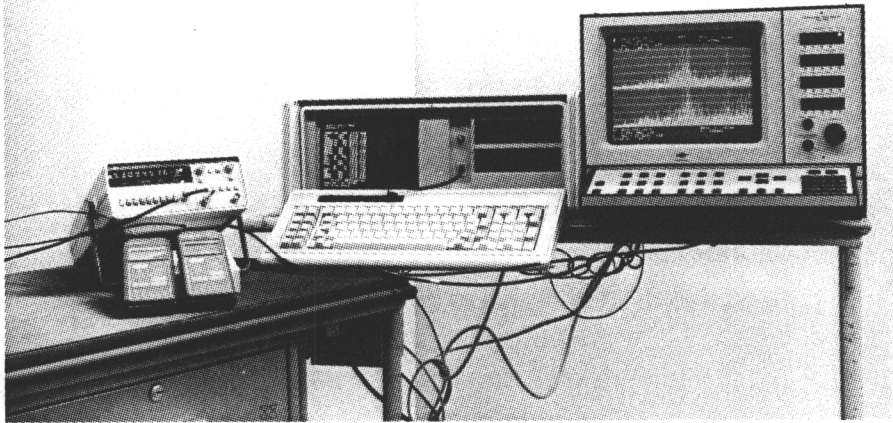


Figure 11. Measurement Equipment

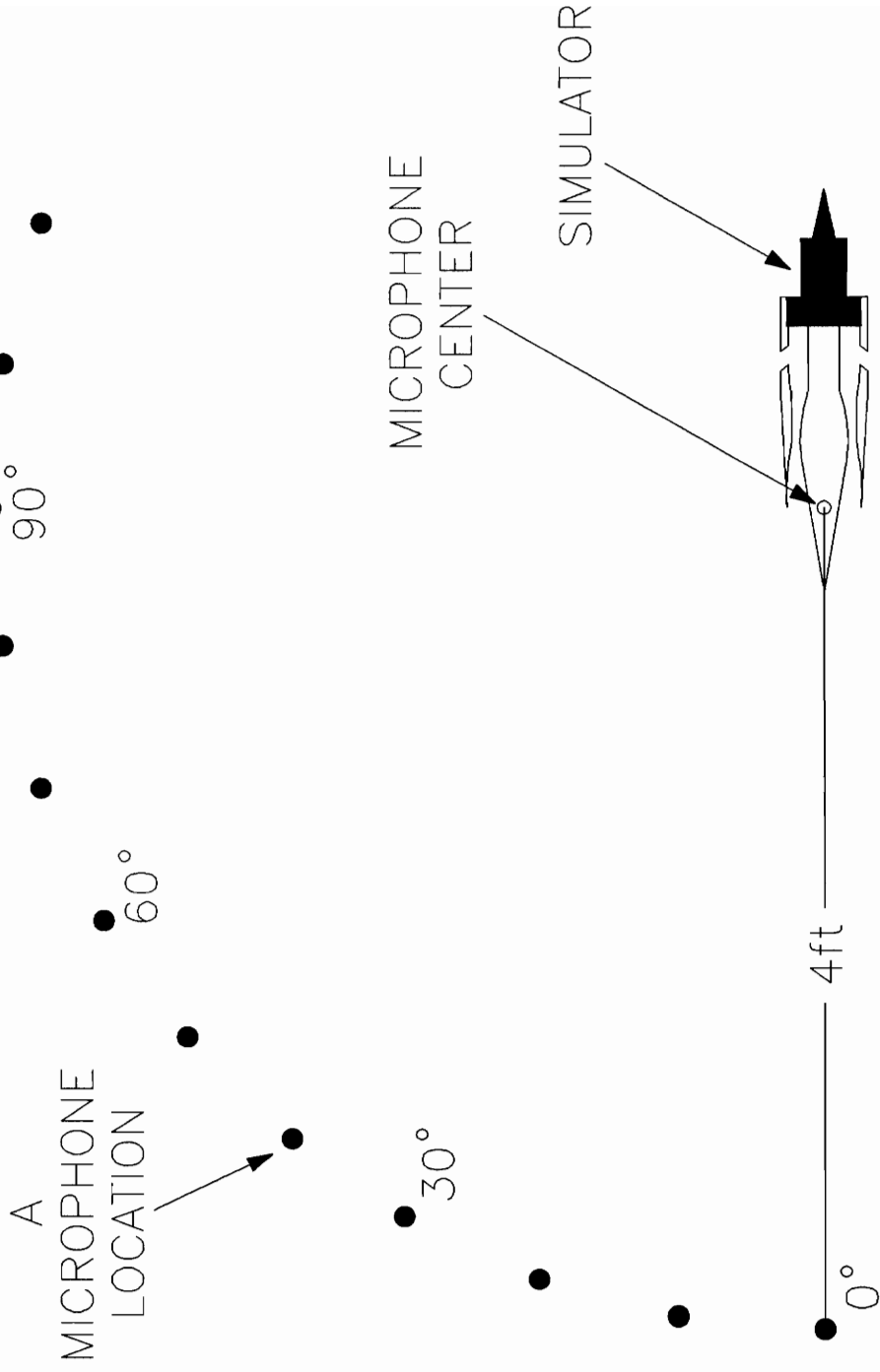


Figure 12. Microphone Layout

microphones were placed 122 cm (4 ft) from the inlet face and positioned at 10° increments from 0° to 110°. The microphones are placed only 122 cm (4 ft) from the inlet face, because the simulator is only 10.4 cm (4.1 in) in diameter. The microphones were not placed above 110°, because the main emphasis of the research is to investigate the forward propagating fan noise.

Initially, there was a concern about possible jet and jet mixing noise. To reduce the jet noise, a 6 m (20 ft) long tube was connected to the exit of the simulator to capture the jet plume. The acoustic results indicated that the jet noise was not influencing the measurements. Therefore, the 6 m (20 ft) long tube was not used again in the experiment.

4.0 Results

The results are divided into aerodynamic and acoustic sections. The aerodynamic results verify that the fan operating conditions are matched. Further, the aerodynamic results show that there is reduced inlet distortion from the modified auxiliary door. The acoustic results will show that the noise has been decreased by the modified door design.

4.1 Aerodynamic Results

4.1.1 Matching Operating Conditions

The area averaged fan pressure ratio is almost identical between the baseline and modified door case. In addition, the fan pressure ratio from the closed door case is very similar to the results from the baseline and modified door configuration. Since the fan rpm and pressure ratio are about the same for all three cases, the three inlet configurations

have the same overall fan mass flow rate. The significance is that all future acoustic comparisons will be done under similar fan operating conditions. The overall area averaged fan pressure ratio is shown in Table 3.

Table 3. Average Fan Pressure Ratio

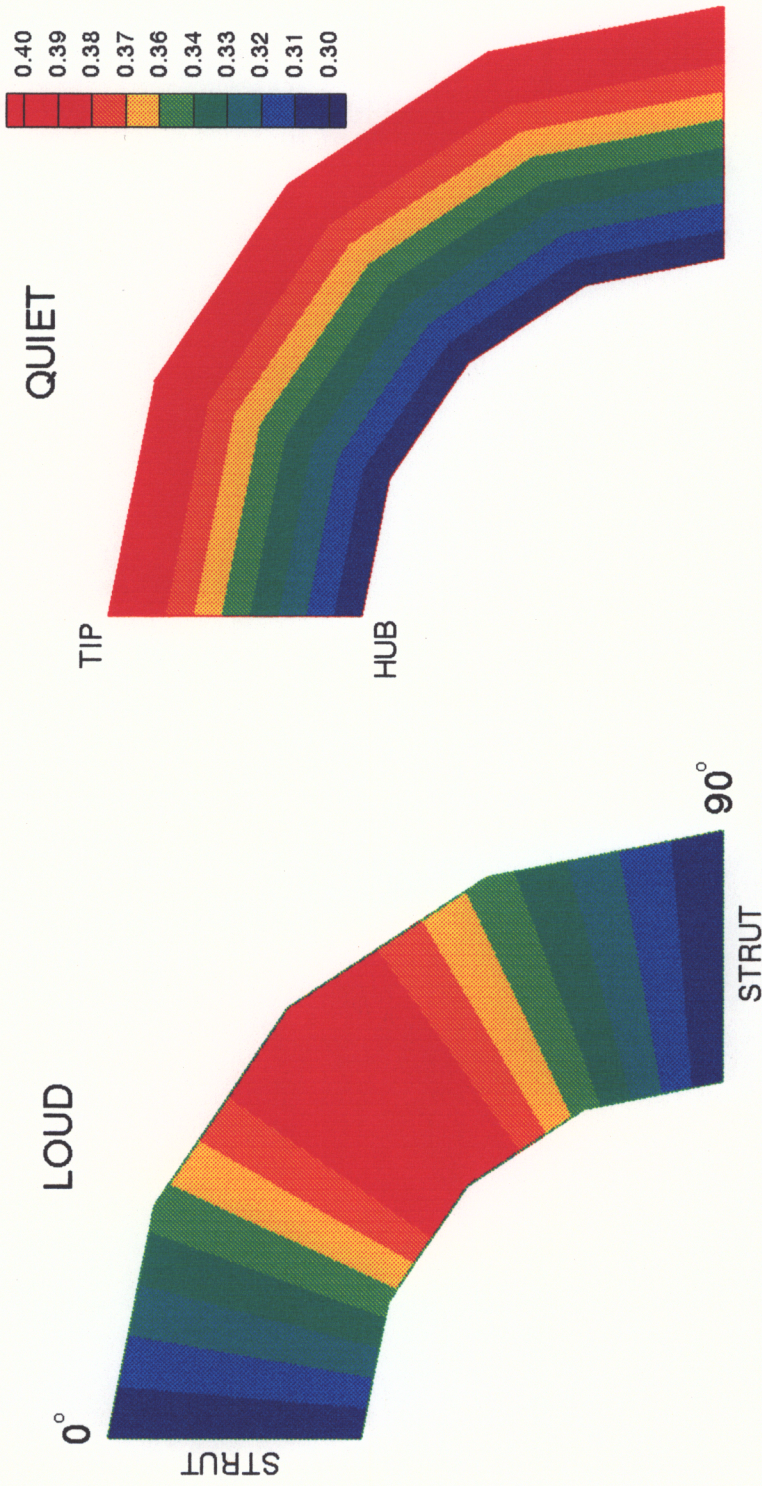
Auxiliary Door	Pressure Ratio
Baseline	1.18
Modified	1.18
Closed	1.19

The difference between all three cases is small. The original purpose for the auxiliary doors is to provide additional air to the engine, but the results show that all three inlet configurations produce almost the same fan pressure ratio, and therefore the same mass flow to the engine. The similar mass flow rate for all three inlet configurations is a result of testing at 58% of the simulator design speed. The advantage is that the closed door acoustic results can be directly compared to the baseline and modified door configuration, because the fan operating conditions are similar between all three cases.

4.1.2 Inlet Distortion

Before presenting the inlet distortion results, it is important to consider how aerodynamics can affect the noise generation. It is crucial to understand the difference between radial and circumferential gradients and their influence on the noise generation. To distinguish the difference, two hypothetical gradient profiles are presented in Figure 13. Figure 13 displays Mach number contours of the flow field at the fan face for both radial and circumferential gradients. Each contour represents a quarter of the inlet at the fan face. The contours represent 0° to 90° with struts located at 0° and 90° . The outside radius represents the location of the pitot-static probe measurements near the fan tip. The inside radius depicts the location of the probe near the fan hub. The contours only represent the area inside the probe measurement locations and therefore do not include the segment of area near the blade tip or hub.

It is important to understand how the gradients in Figure 13 affect noise generation. Contour **B** demonstrates gradients only in the radial direction. Any location on a fan blade as it traverses from 0° to 90° is exposed to a constant Mach number in the direction of travel. For example, a point on the blade near the tip will only process air with a Mach number in the red region of about 0.39. Radial gradients therefore produce steady blade loading as the blade rotates. This steady blade loading will reduce the amount of noise generation. Contour **A** demonstrates gradients only in the circumferential direction. As a point on a fan blade at a given radius traverses from 0° to 90° , it will experience varying inlet Mach numbers. For example, any point on the blade will now



A: CIRCUMFERENTIAL DISTORTION B: RADIAL DISTORTION

Figure 13. Hypothetical Mach Number Contours at Fan Face

be exposed to Mach numbers ranging from 0.30 at 0°, up to 0.40 at 45°, and then back down to 0.30 at 90°. This variance creates an unsteady blade loading, which will increase the noise generation when compared to case B.

Figure 14 shows the inlet Mach number distribution at the fan face for the baseline and modified case, as measured in the experiment. On the outside of the modified case, the two tick marks show the location of the auxiliary inlet door. As mentioned, the strut is removed to make the measurements at 0°. When the strut is removed, there is an increase in flow area which should decrease the measured Mach number. This increase in area is the suspected cause for the slightly lower Mach numbers near 0° and 90°. Lower Mach numbers at 0° and 90° are therefore expected in all measured cases. The important aspect of the modified case is the more uniform Mach number distribution. In the modified case most of the area is in the 0.33 to 0.36 Mach number range. This uniform region produces steady blade loading, which in turn reduces the noise generation.

The baseline case in Figure 14 has significant differences from the modified case. There are no uniform regions, and in particular there are gradients in the circumferential direction. The tick marks on the baseline case at 20° and 70° indicate the auxiliary door location. The regions suspected of generating the most sound are near the blade tip in the 0° to 20° range and in the 70° to 90° range. When the blade tip traverses from 0° to 20° the Mach number changes from 0.30 to 0.40. The 0° to 20° region and the 70° to 90° region near the blade tip both have large gradients in the circumferential direction, and are therefore suspected of being a predominant noise source. Also, at the blade tip, the blade speed is higher which causes any disturbance to produce more noise. Other

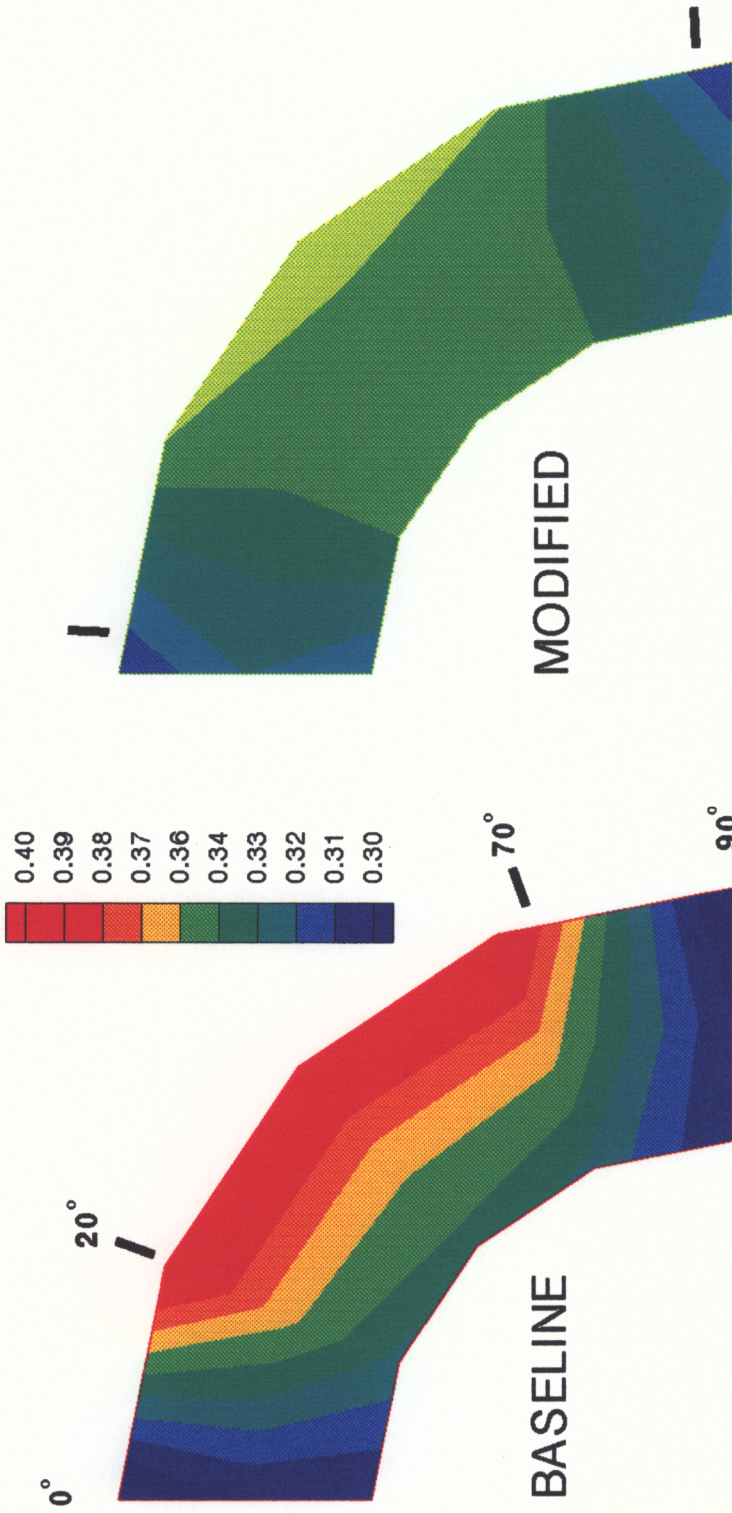


Figure 14. Inlet Mach Number Distribution at Fan Face

disturbances at the blade tip include secondary flow and tip leakage.

The closed door Mach number distribution is shown in Figure 15. The results show significant radial gradients, but there are minimal changes in the circumferential direction. The only changes in the circumferential direction are at 0° and 90° which are attributed to the strut removal. The lower Mach numbers at the hub and tip are caused by the build up of the boundary layer in the inlet. The small gradient in the circumferential direction will therefore generate minimal noise.

When comparing the Mach number distribution from all three cases, the baseline door configuration is shown to have the greatest circumferential distortion. Table 4 quantifies this distortion by listing the Mach number distortion in the circumferential direction. To calculate the circumferential distortion, the formula $(M_{MAX} - M_{MIN})/M_{AVG}$ is used to calculate a distortion value for the measurements taken at one radius. The above formula is then repeated on the measurements taken at the other two radii. To calculate the overall circumferential distortion, the three distortion values are then averaged by area weighting. By comparing the Mach number circumferential distortion results from all three cases, the baseline door configuration is suspected of generating the most noise. The closed door case is expected to produce the least amount of sound. The modified door configuration is expected to generate sound on a level between the baseline and closed door case. The above hypotheses are confirmed by the acoustic results to be presented later.

Other aerodynamic results also substantiate similar trends. For instance, the inlet mass flow distribution to the fan face in Figure 16 shows that the baseline configuration

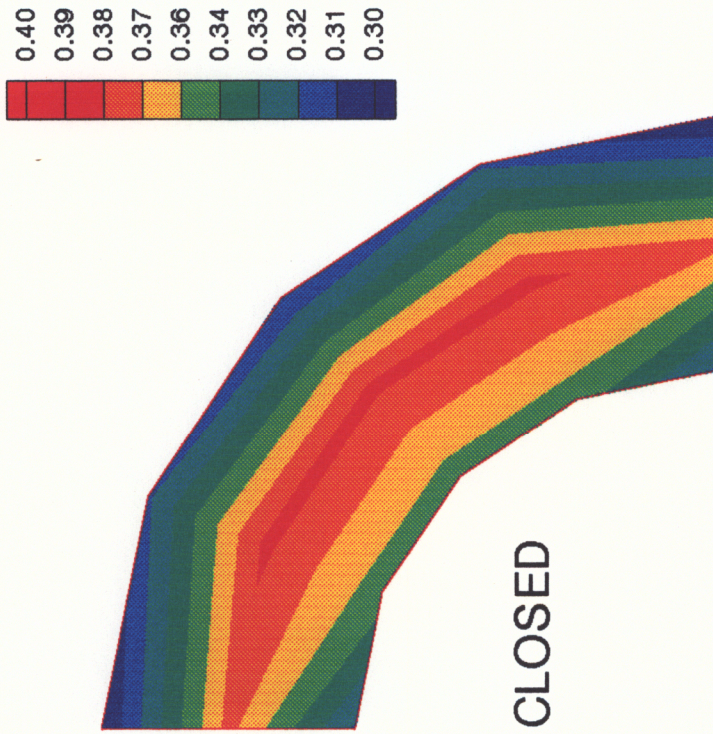


Figure 15. Closed Door Mach Number Distribution at Fan Face

Table 4. Mach Number Distortion in the Circumferential Direction

Auxiliary Door	Circumferential Distortion
Baseline	0.22
Modified	0.11
Closed	0.06

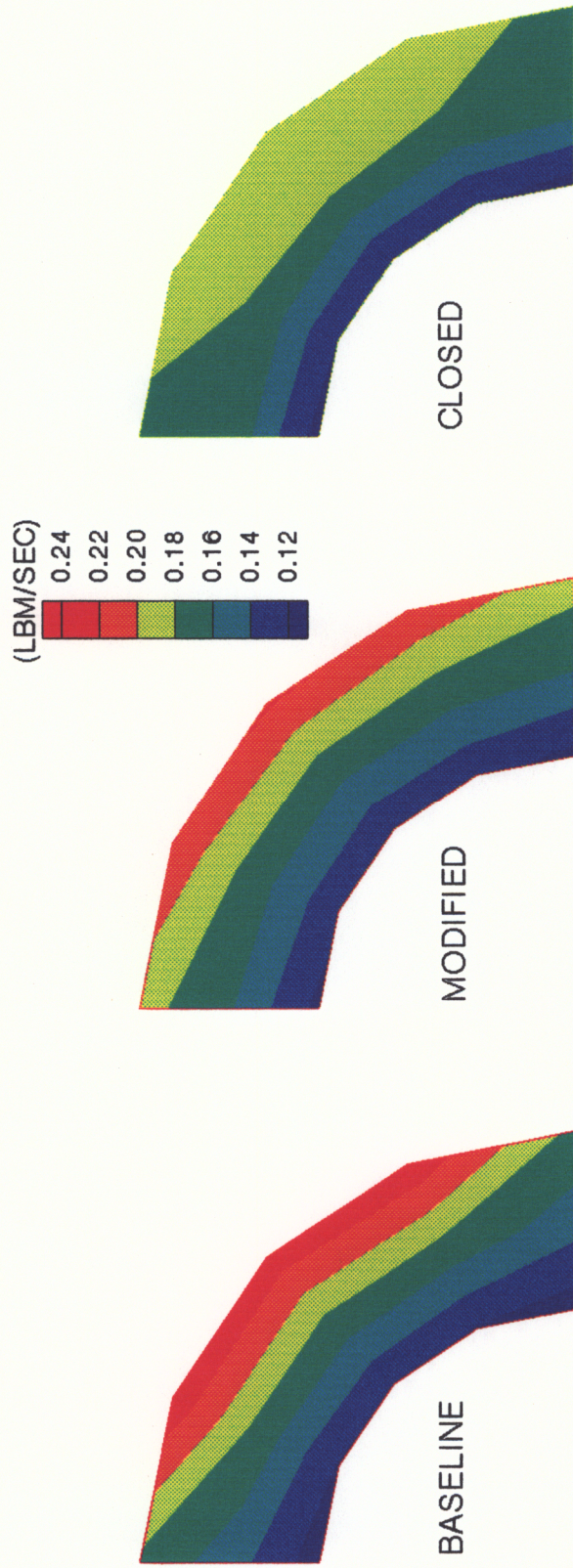


Figure 16. Inlet Mass Flow Distribution

again has the highest distortion in the circumferential direction. Figure 17 shows the inlet total pressure recovery at the fan face. The figure presents the inlet total pressure as a percentage of the ambient surrounding total pressure. The contours indicate inlet total pressure losses. The closed door case has high losses at the inside and outside radii, which is caused by the build up of the boundary layer. The modified case has some slight losses at the outside radius. The baseline case has a large loss of 10% at the 45° measurement location at the outside radius. This high loss is most likely caused by the baseline door. This loss also increases the circumferential distortion, producing an unsteady blade loading, which increases noise.

Figure 18 shows another distribution with the contour of the fan pressure ratio at the fan exit. Except for the measurements taken at 22.5°, the modified and closed door case each have minimal changes in the circumferential direction. The higher fan pressure ratio at these locations is probably caused by the strut in the inlet. The strut is located before the fan at 0°. The strut is presumed to create a wake which in turn causes the fan to process air with a low mass flow region. A lower mass flow region when processed by the fan will tend to create a region of higher fan pressure ratio. When air is processed by a fan, it is turned in the rotor and receives a shift in the circumferential direction. A simple analysis of the fan and its operating conditions indicates that the air would receive a shift in the circumferential direction of about 20°. This shift is consistent with the results shown in the contour plots. The baseline door case also has a higher pressure ratio at 22.5°, but there are low measurements at 45° and then high measurements at 67.5°. Once again, as expected, the baseline case is not as uniform in the circumferential

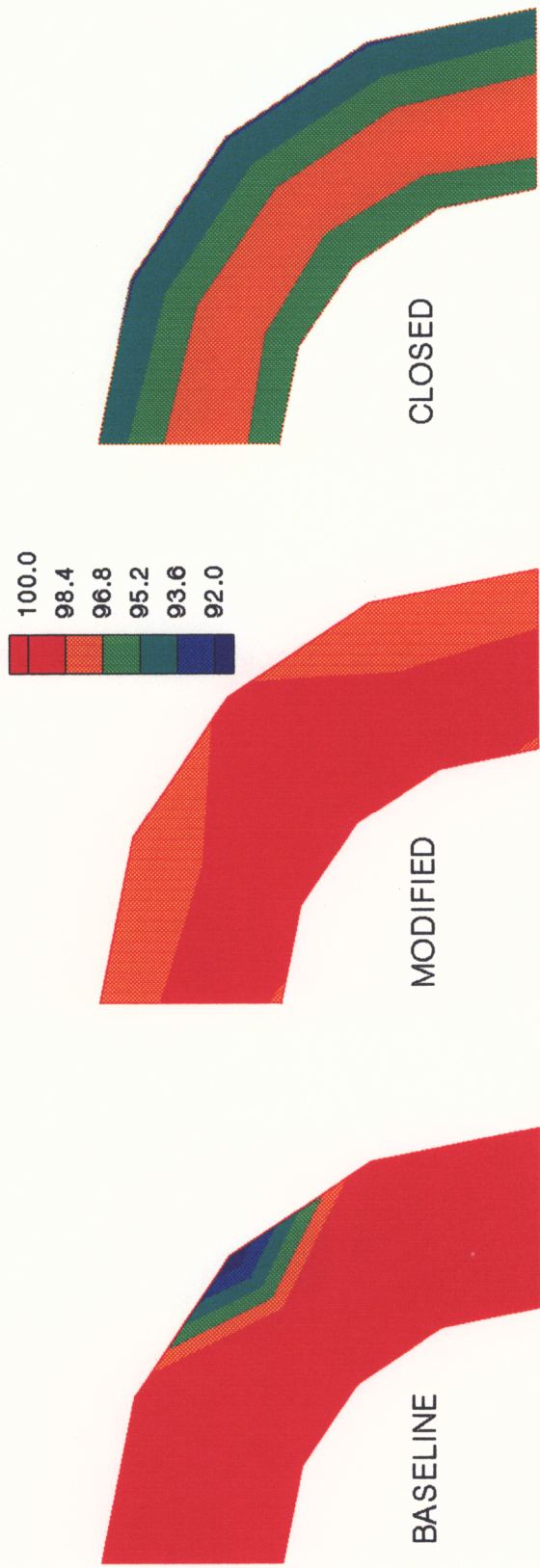


Figure 17. Inlet Fan Face Total Pressure Recovery (%)

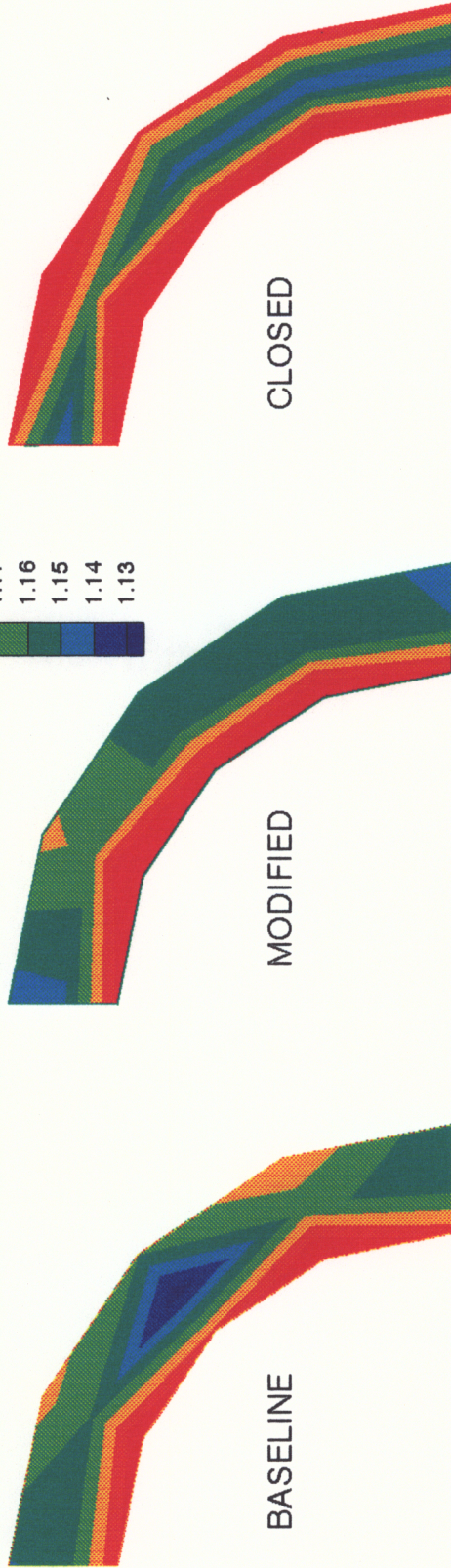


Figure 18. Fan Pressure Ratio Distribution at Fan Exit

direction when compared to the other two cases.

4.1.3 Inlet Aerodynamic Performance

The inlet Mach numbers at the different axial stations, for the baseline and closed door case, are seen in Figure 19. Opening the baseline doors has a large effect on the throat station Mach number. The Mach number drops from 0.83 for the closed case to 0.32 for the baseline case. Although not shown in a figure, the throat station Mach number is 0.50 for the modified door case. Previous research from reference 2 indicates that Mach numbers of 0.5 or below are not expected to exhibit the choking effect. Since the Mach number in the throat for the closed case is above 0.5, there will be a choking effect at the throat station which attenuates the noise radiation. Figure 20 shows the corresponding inlet total pressure recovery for the baseline and closed door case. The inlet total pressure recovery for the closed door case is slightly lower at the fan station, especially near the hub and tip radial positions. Again, this difference is due to the build up of the boundary layer in the closed door case.

Based on an analysis of the aerodynamic results, it was estimated that the design objective to employ the choking effect in the modified auxiliary door itself has not been achieved. This failure is caused by the fan not pulling a large enough mass flow (due to testing at 58% design speed). The Mach number in the auxiliary doors was not directly measured. The door mass flow was approximated by subtracting the mass flow through

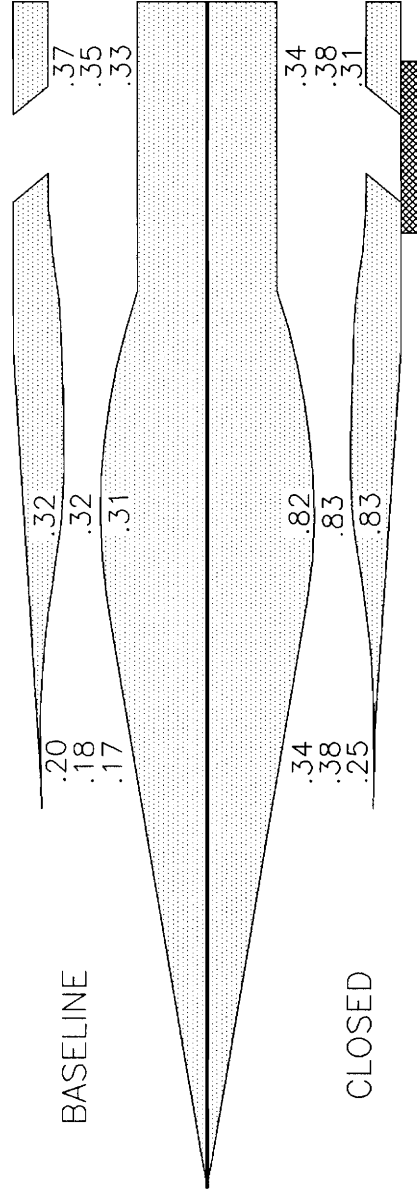


Figure 19. Baseline vs. Closed Inlet Mach Numbers

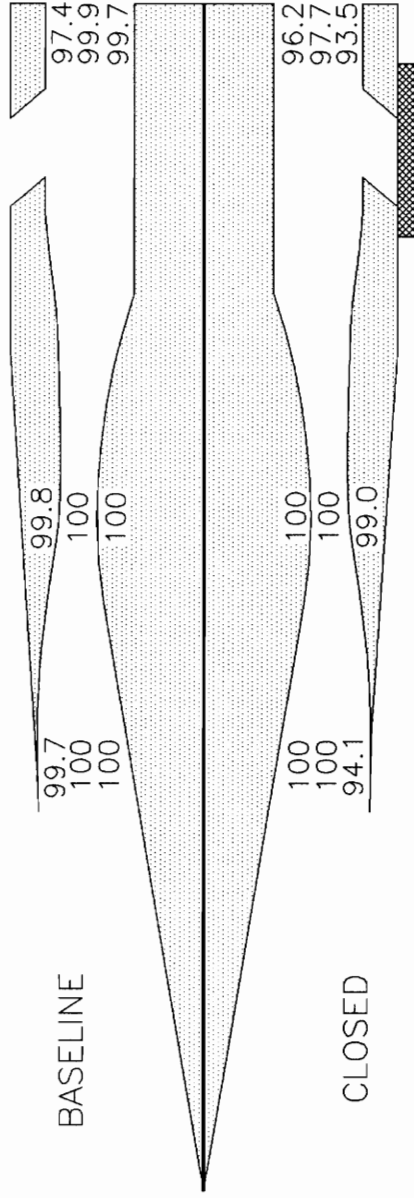


Figure 20. Inlet Total Pressure Recovery (%)

the throat from the mass flow through the fan. Then, the Mach number in the auxiliary inlet doors was isentropically calculated. The results indicate the baseline door to have a Mach number of 0.23 and the modified door a Mach number of 0.27. As mentioned before, the throat Mach numbers are 0.32 and 0.50 for the baseline and modified door case respectively. Since no Mach numbers are above 0.5, there are no expected choking effects anywhere in either the baseline or modified case.

4.2 Acoustic Results

4.2.1 Sample Spectrum Data

The sample data is a narrow band spectrum analysis plotting the sound pressure level versus the frequency. Figure 21 compares data from the baseline and modified case at 10°. The BPF tone at about 15 kHz is distinct and at least 10 dB above the broadband noise. The three tones shown in the baseline case from 3 to 11 kHz are the on-set of multiple pure tones. These initial multiple pure tones are observed at all angles.

A comparison of the baseline and closed door case taken at 70° is shown in Figure 22. Again, in the baseline case the multiple pure tones are evident throughout the spectrum. The important difference between the baseline and closed door case is the change in the shape of the broadband noise. The baseline case broadband noise changes little with frequency while the closed door broadband noise tends to vary more with the

BASELINE

(10 degrees)

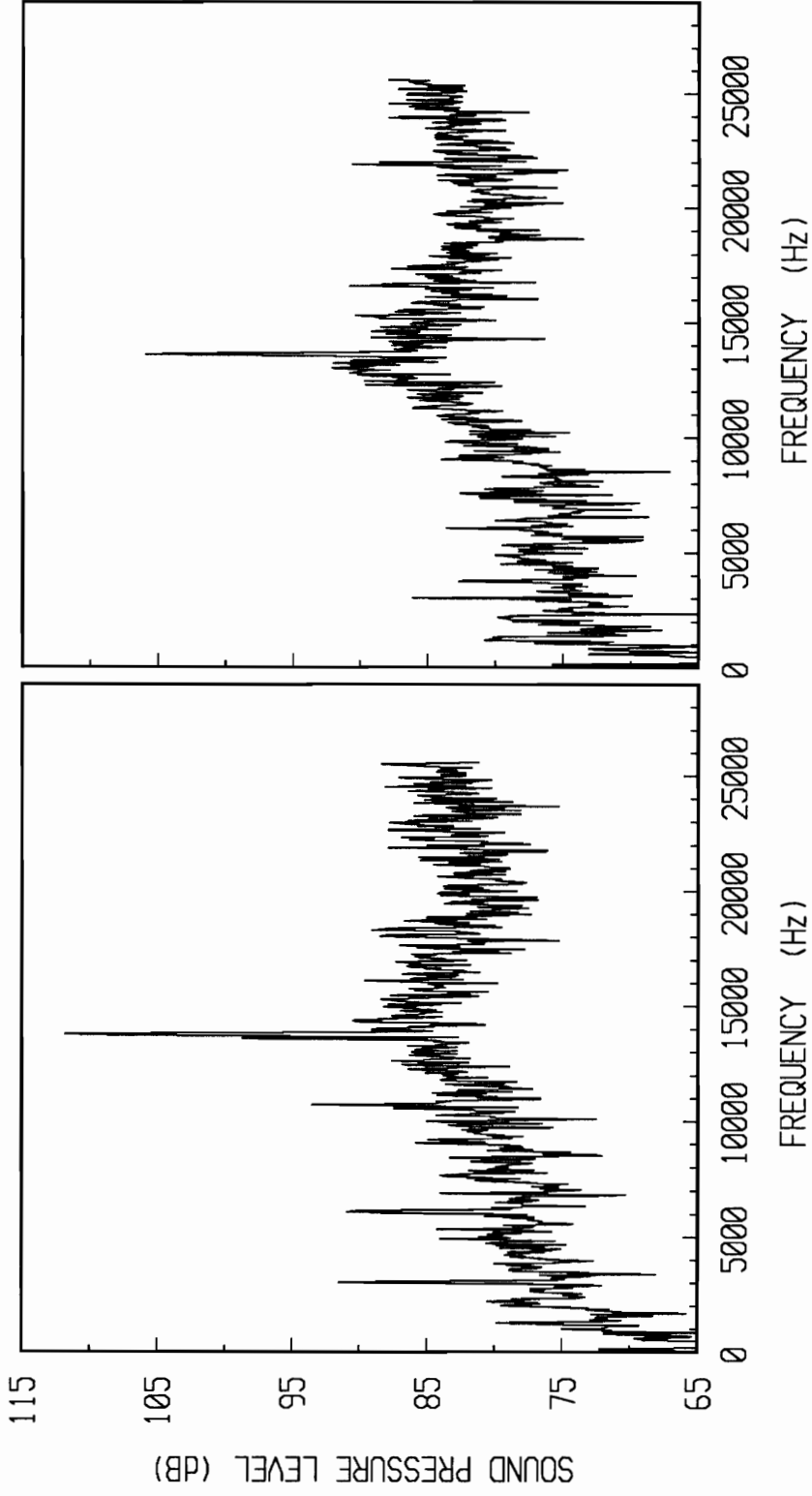


Figure 21. Sample Data (Baseline vs. Modified)

BASELINE (70 degrees) CLOSED

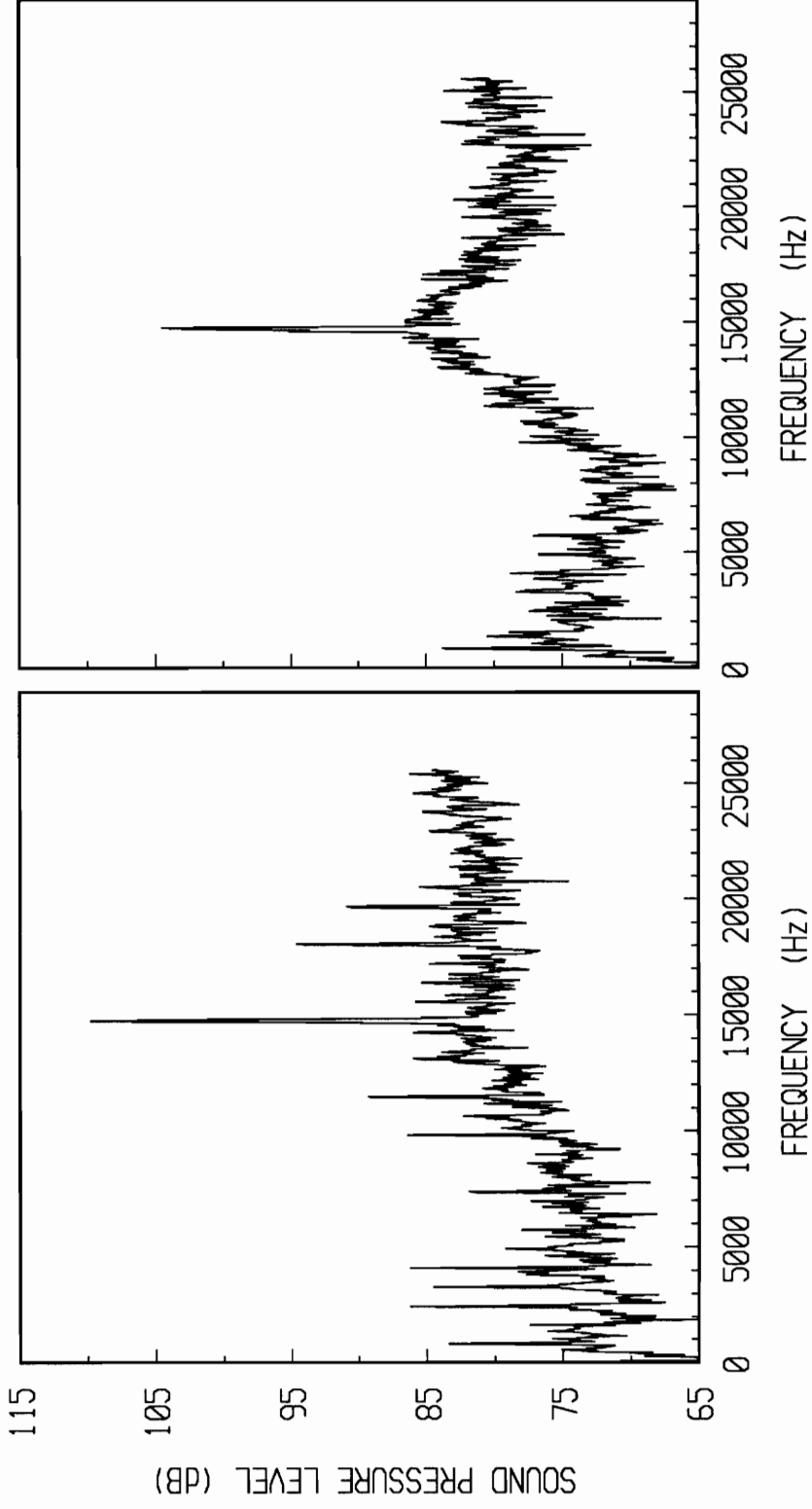


Figure 22. Sample Data (Baseline vs. Closed)

frequency. This change in the shape of the broadband noise is observed at all the measured angles. The reason for the change in the broadband noise shape is not known. Not enough data has been taken on the broadband noise to draw any conclusions. A preliminary analysis though does indicate that the broadband noise from the baseline case is greater than the broadband noise from either the modified or closed door case.

4.2.2 BPF Tone versus Angle

Figure 23 is the key result that compares the baseline and modified auxiliary inlet doors. The plot shows the sound pressure level of the BPF tone versus the angle. The greatest reduction in the tone is observed in the forward sector. The tone is reduced by an average of over 6 dB in the 0° to 40° range. The primary cause for this reduction can be attributed to the modified auxiliary door decreasing the circumferential distortion at the fan face. Thus, it has been shown that the modified auxiliary door configuration is successful in reducing the BPF tone. At the higher angles the two results tend to converge. The two BPF tone levels also tend to increase in the 90° to 110° range. Uncertainty bands are included in the figure at two angles. The uncertainty bands show a calculation of one standard deviation, from the average, of the ten measurements taken at each angle. The uncertainty is acceptable, but it can be reduced by improving the test facility.

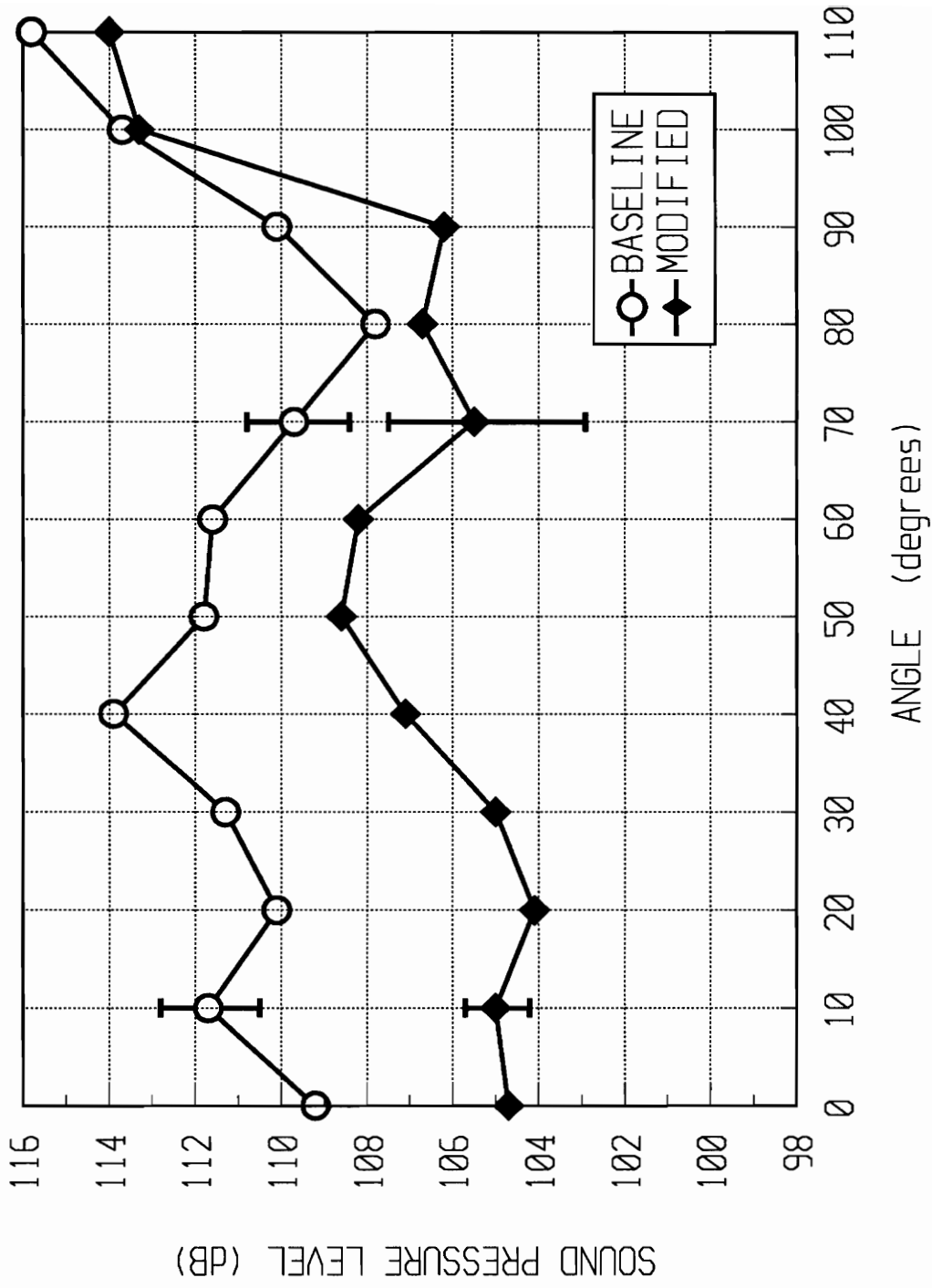


Figure 23. BPF Tone vs. Angle (Baseline vs. Modified)

A comparison of the baseline and closed door case is shown in Figure 24, along with two uncertainty bands. The greatest difference is also in the 0° to 40° range with a reduction in the tone by an average of 10 dB. The closed door case reduction in tone can be attributed to three factors: the reduced circumferential distortion to the fan face, the choking effect at the throat station, and no direct radiation path through an auxiliary door. At the 10° microphone location the choking effect at the throat station has been measured to be about 4 dB, (see Appendix A for a description of the measurement). The choking effect is shown in Appendix A to reduce both the BPF tone and broadband noise. From a preliminary analysis the choking effect is more predominant at the lower angles. To compare the BPF tone results from all three inlet configurations, Figure 25 shows a polar plot of the BPF tone.

4.2.3 Comparison with Previous Research

Figure 26 is a comparison with some of the previous research conducted at NASA Lewis. This figure is a plot of the difference in the BPF tone (baseline minus closed) versus the angle. There is good agreement from 0° to 70° considering the Reynolds number difference of the two models, and that the two cases were not performed under the exact same conditions. At NASA Lewis the research was performed in a completely different test facility. NASA Lewis used an anechoic wind tunnel, while at Virginia Tech the tests were conducted in an outdoor facility. In addition, the two test cases were not

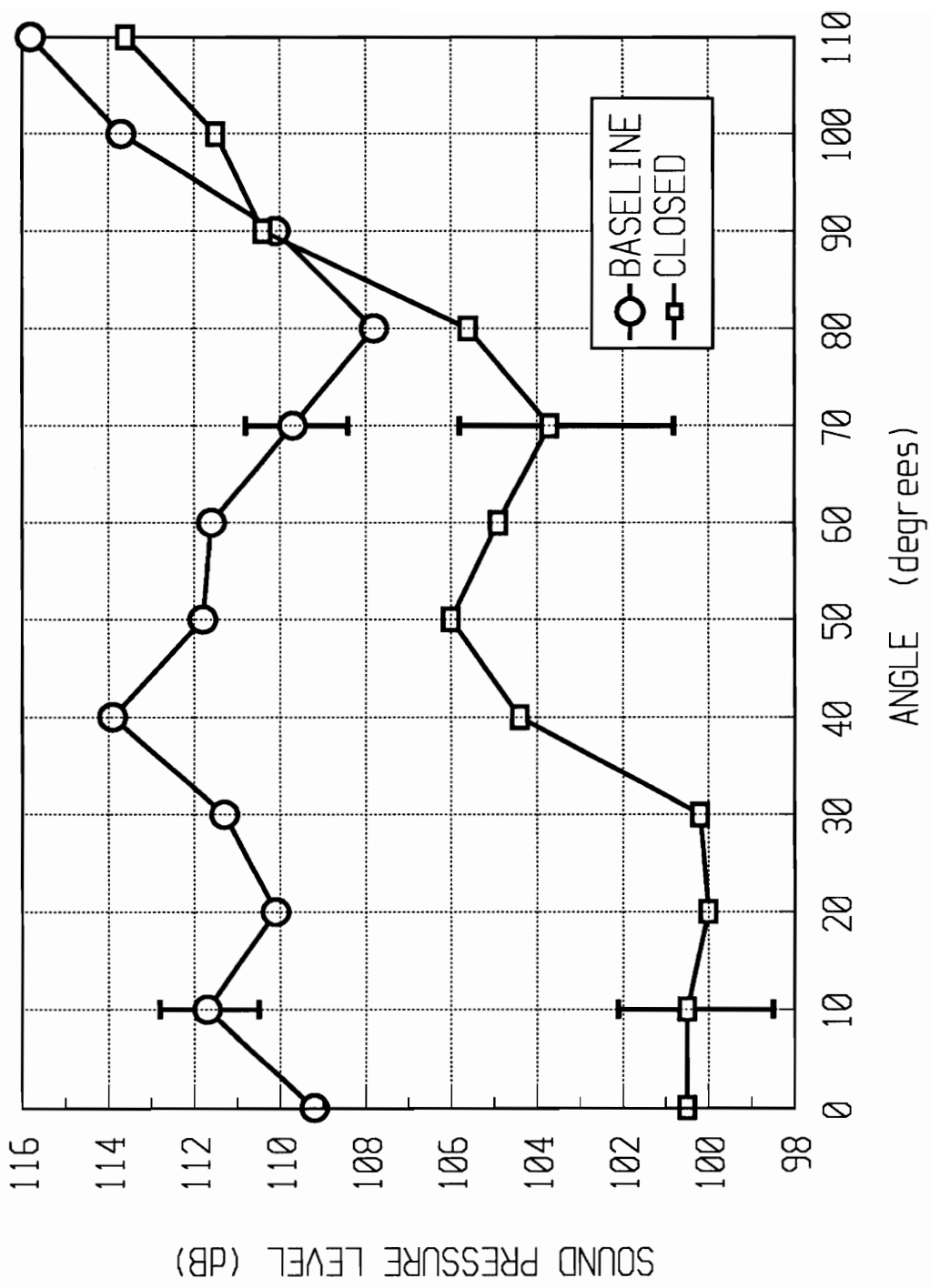


Figure 24. BPF Tone vs. Angle (Baseline vs. Closed)

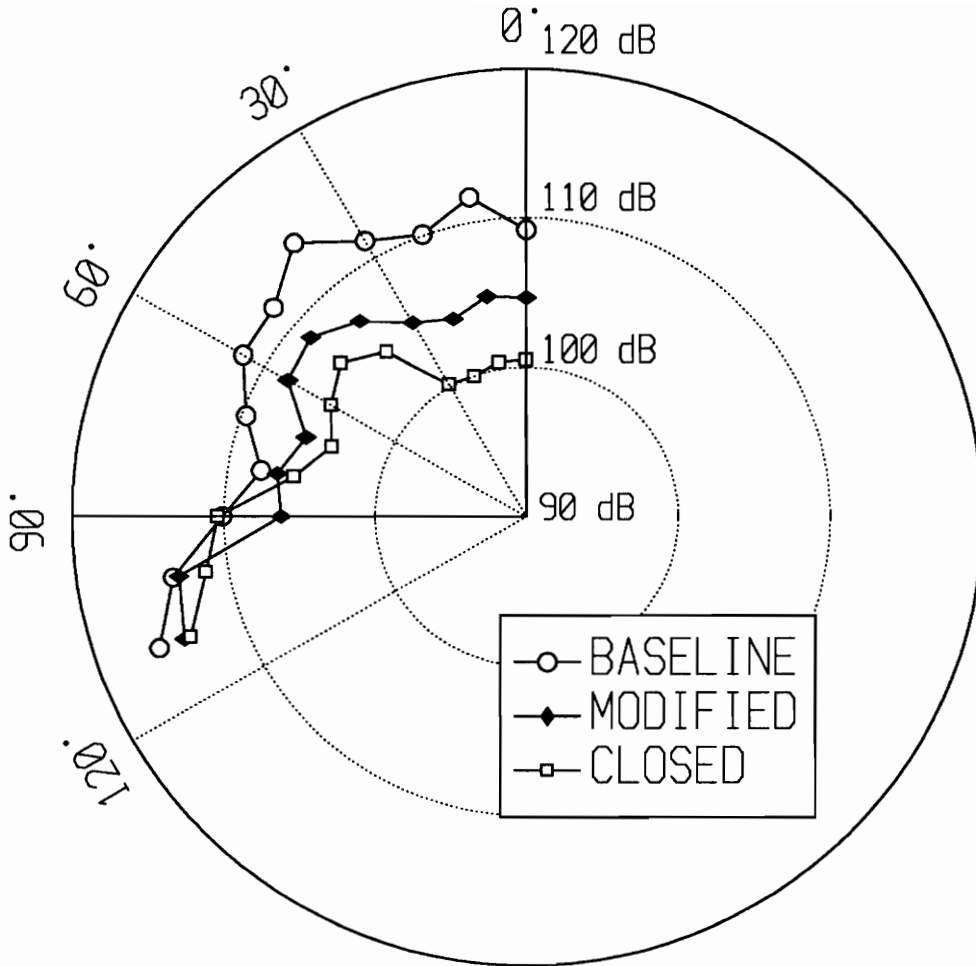


Figure 25. Polar Plot of BPF Tone

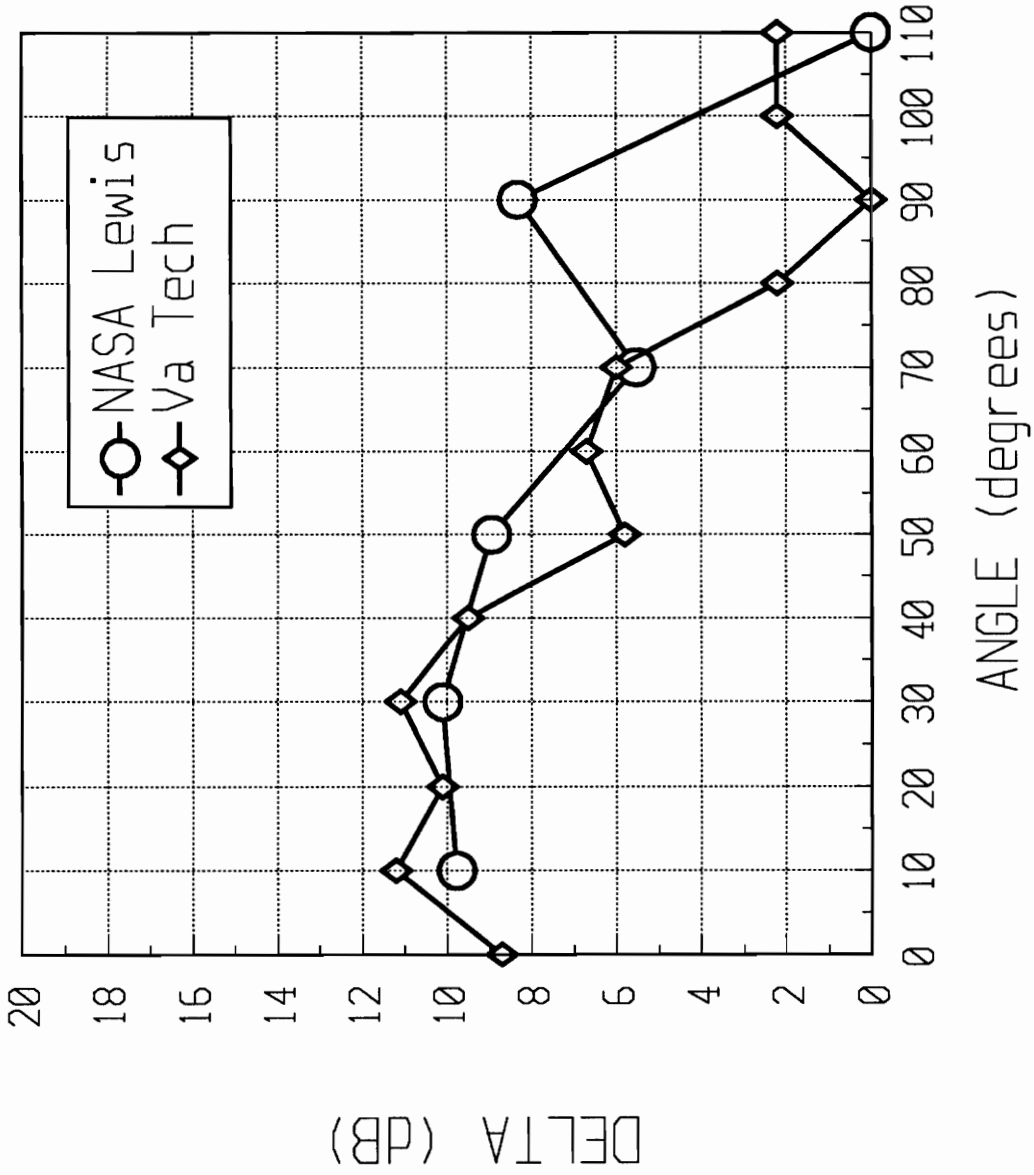


Figure 26. Delta BPF Tone (Baseline Minus Closed)

performed with the exact same inlet configurations, in the NASA Lewis case the centerbody was extended forward. However, the throat station Mach numbers are similar, and therefore both cases should employ similar choking effects making the tests acceptable for comparison. The Reynolds number difference will be discussed in the next chapter. Figure 26 demonstrates that the 10.4 cm (4.1 in) simulator can produce results with trends similar to larger and more expensive test programs.

5.0 Conclusions and Recommendations

5.1 Conclusions

The main objective of this research was to reduce the noise radiating from a supersonic inlet. A series of experiments was performed with a small-scale model of an axisymmetric, mixed-compression, supersonic inlet connected to a turbofan engine simulator. By modifying the auxiliary inlet door, the forward propagating fan BPF tone noise was reduced by an average of 6 dB in the 0° to 40° sector when compared to the original baseline design of the auxiliary door. The modified auxiliary inlet door was designed to employ a choking effect in the door and to reduce the distortion to the fan face. The choking effect in the modified door was not achieved, because the simulator was tested at 58% design speed. As mentioned earlier, testing at 58% design speed generates noise in the pure tone region, which is expected to be a significant noise source during the aircraft landing approach. A reduction in distortion has been achieved and was

shown by: the Mach number, the mass flow, the inlet total pressure recovery, and the fan pressure ratio results. The primary cause for the reduction in BPF tone noise is attributed to the modified auxiliary door decreasing the circumferential distortion at the fan face. Thus, it has been shown that the main objective of this research has been accomplished.

A comparison of the baseline and closed door case shows that the BPF tone is an average of 10 dB higher in the 0° to 40° range for the baseline case. This result is consistent with previous research. The decrease in BPF tone is attributed to three factors: the reduced inlet distortion at the fan face, the choking effect at the throat station, and no direct noise radiation path through an auxiliary inlet door.

The Reynolds number is an important experimental consideration in testing. Table 4 compares the Reynolds number between the 10.4 cm (4.1 in) simulator, P-inlet tested at NASA Lewis, and an actual flight engine.

Table 5. Reynolds Number Comparison

Reynolds Number	Inlet	Scale
1.7 x 10 ⁶	Virginia Tech, 10.4 cm (4.1 in)	1/14
7.6 x 10 ⁶	NASA Lewis, P-inlet 50.8 cm (20 in)	1/3
22.7 x 10 ⁶	Actual Flight Engine	1

A potential problem is that small-scale model results might not correctly predict the noise when compared to an actual full size engine with a larger Reynolds number. This problem is of a lesser concern because the main emphasis here is on trends and noise mechanisms, instead of results that can be directly used to predict full scale noise. An important aspect to note is that the cost of an experiment is usually proportional to the Reynolds number being tested. Even though the supersonic inlet tested was 1/5 the size of the previously tested P-inlet, the results are similar. These results demonstrate that the 10.4 cm (4.1 in) simulator can produce results similar to larger and more expensive test programs.

5.2 Recommendations

From the results presented in this paper, there is a need to better understand how circumferential distortion effects the noise generation. The results have shown that the baseline door increases the BPF tone noise in the forward sector. This increase in noise is attributed to the baseline door increasing the circumferential distortion at the fan face. The aerodynamic results show the baseline configuration to have both inlet total pressure and Mach number circumferential distortion. The current need is to understand whether inlet total pressure or Mach number circumferential distortion produces the most noise. Currently, it cannot be determined which type of circumferential distortion generates the most noise.

With the three inlet configurations, the first recommendation is to test with the simulator running at 100% design speed. The increased speed should provide enough mass flow to employ the choking effect in the modified auxiliary inlet door. This increased speed will provide flexibility in the testing program to investigate more combination effects. The purpose is to better understand the influence of the centerbody location on the auxiliary doors to determine the optimum position for aerodynamics and acoustics. At the higher simulator engine speed, the blade tip will be supersonic causing the noise generated to be in the multiple pure tone region. The multiple pure tones are expected to be a significant noise source during the aircraft take off condition. The multiple pure tones could have a dramatically different effect on the noise mechanisms and radiation from the inlet.

An overall recommendation is to more effectively integrate aerodynamics and acoustics. Little is known about the noise mechanisms in a supersonic inlet. Computational Fluid Dynamics (CFD) should be used to calculate the aerodynamic effects of opening the auxiliary inlet doors. CFD can assist in studying the aerodynamic effects of different door geometries to choose an optimum shape before any acoustic measurements are taken, thereby reducing time and cost. The above will enhance the understanding of the physics involved and therefore increase the knowledge of how aerodynamics and acoustics interact.

There are many possible tests that could be conducted. Although not tested, the boundary layer bleed system is a noise source that must be addressed. Another area of interest is the engine, inlet, and airframe installation effects. How will the sound radiating

from a supersonic inlet interact with the fuselage, wing, or airframe? In previous research, a test program studied different strut configurations. The small inlet is ideal to perform these various parametric studies.

Altogether, testing of the small scale inlet is inexpensive and can produce preliminary results in a short period of time.

Appendix A. Choking Effect

The choking effect for the closed door case has been measured by translating the centerbody forward. Translating the centerbody forward increases the throat area in the inlet, which in turn decreases the throat Mach number. Figure 27 shows the effect of the centerbody position on the Mach number. At the top half of the figure, the centerbody is extended 70% of the maximum distance, $x/R_1 = 1.57$. The bottom half displays the previously shown results, with the centerbody extended 0%. The 0% extension case will employ the choking effect, because the Mach number is 0.83 at the throat station. When the centerbody is extended forward, the Mach numbers are about 0.44 and 0.51 for the throat and lip station respectively. Since the Mach numbers for the 70% case are not substantially over 0.5, there are no expected choking effects for this configuration.

The choking effect reduces both the broadband and BPF tone noise. Figure 28 shows the choking effect on the broadband noise. The 0% case reduces the broadband noise in the 8 to 25.6 kHz range by about 1.5 dB, (this reduction is for the 10° microphone location). Figure 29 shows the choking effect on the BPF tone for the 10° microphone location. The 0% case reduces the BPF tone by 4.3 dB. As mentioned previously, the choking effect is more predominant at the lower angles. A microphone

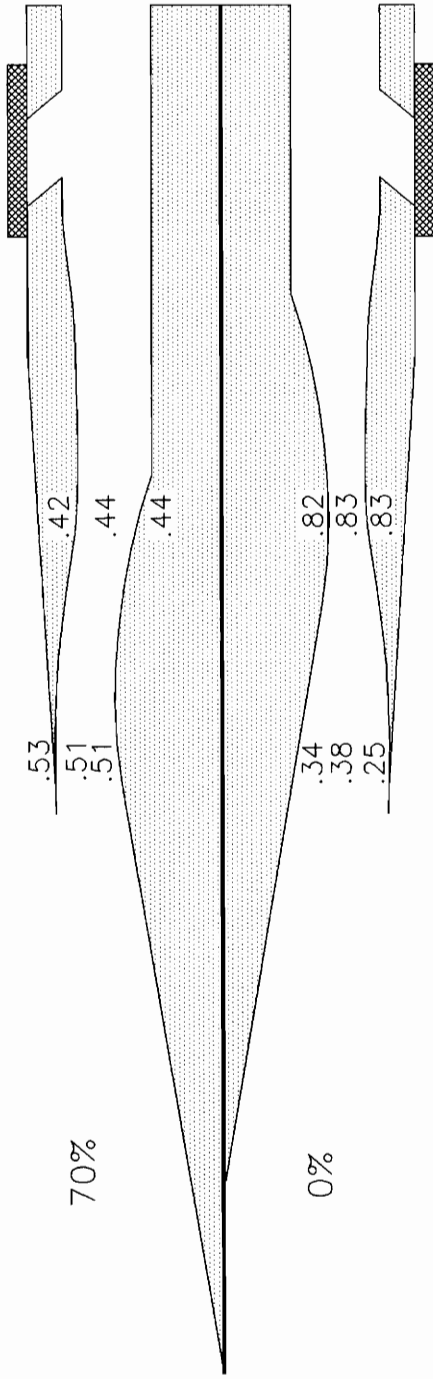


Figure 27. Centerbody Effect on the Mach Number

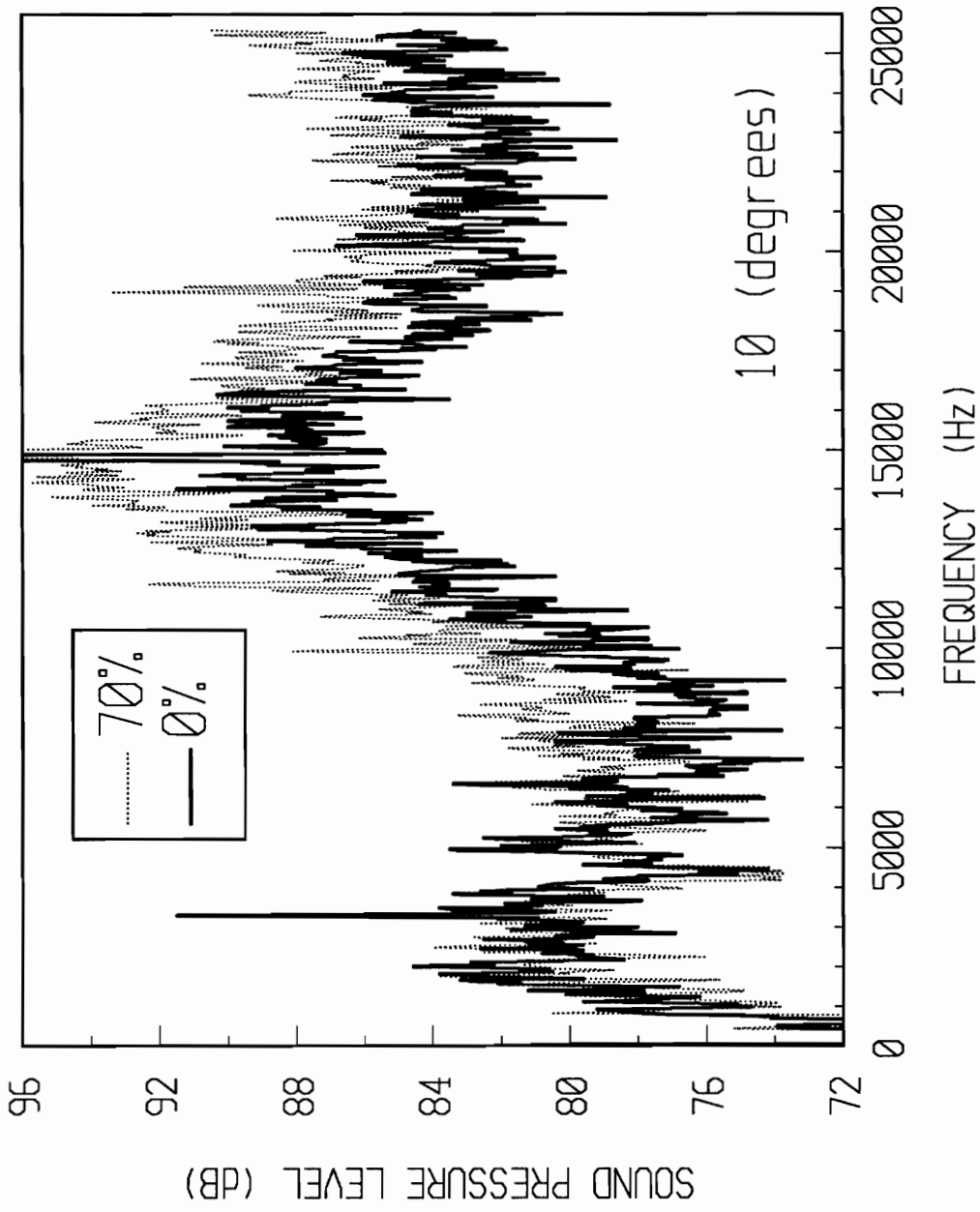


Figure 28. Choking Effect on the Broadband Noise

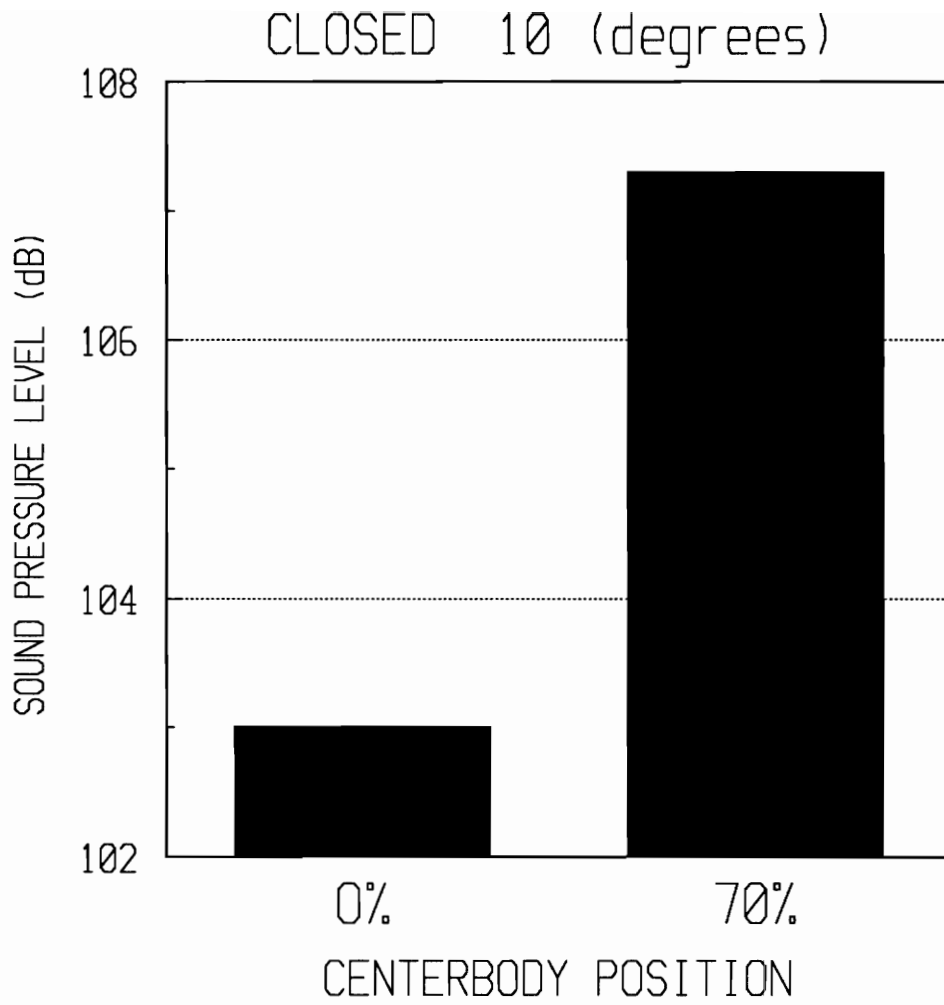


Figure 29. Choking Effect on the BPF Tone

placed at 60° measured no change in the BPF tone with respect the centerbody position. There also seems to be no change in the broadband noise at 60° . Therefore, the choking effect is only present at the lower angles.

References

1. Trefny, C. J., Wasserbauer, J. W., "Low-Speed Performance of an Axisymmetric, Mixed-Compression, Supersonic Inlet With Auxiliary Inlets," NASA TP-2557, February 1986.
2. Woodward, R. P., Glaser, F. W., Lucas, J. G., "Low Flight Speed Acoustic Results for a Supersonic Inlet with Auxiliary Inlet Doors," *AIAA Paper 83-1415*, June 1983.
3. Koncsek, J. L., "Transonic and Supersonic Test of a Mach 2.65 Mixed-Compression Axisymmetric Intake," NASA CR 1977, March 1972.
4. Sorensen, N. E., Bencze, D. P., "Possibilities for Improved Supersonic Inlet Performance," *AIAA Paper 73-1271*, November 1973.
5. Smeltzer, D. B., Sorensen, N. E., "Analytic and Experimental Performance of Two Isentropic Mixed Compression Axisymmetric Inlets at Mach Numbers 0.8 to 2.65," NASA TN D-7320, June 1973.
6. Syberg, J., Turner, L., "Supersonic Test of a Mixed-Compression Axisymmetric Inlet at Angles of Incidence," NASA CR-165686, April 1981.
7. Wasserbauer, J. F., Cubbison, R. W., Trefny, C. J., "Low Speed Performance of a Supersonic Axisymmetric Mixed Compression Inlet with Auxiliary Inlets," *AIAA Paper 83-1414*, 1983.
8. Ball, W. H., Pickup, N., "Low Speed Performance and Acoustic Tests of an Axisymmetric Supersonic Inlet -Phase One Tests with Auxiliary Doors Closed," NASA CR-172390, October 1984.
9. Bangert, L. H., Burcham, F. W., Mackall, K. G., "YF-12 Inlet Suppression of Compressor Noise: First Results," *AIAA Paper 80-0099*, January 1980.

10. Bangert, L. H., Feltz, E. P., Godby, L. A., Miller, L. D., "Aerodynamic and Acoustic Behavior of a YF-12 Inlet at Static Conditions," NASA CR-163106, January 1981.
11. Topol, D. A., Holhubner, S. C., Mathews, D. C., "A Reflection Mechanism for Aft Fan Tone Noise from Turbofan Engines," *AIAA Paper 87-2699*, October 1987.
12. Topol, D. A., "Rotor Wake/Stator Interaction Noise-Predictions Versus Data," *AIAA Paper 90-3951*, October 1990.
13. Tyler, J. M., Sofrin, T. G., "Axial Compressor Noise Studies," *SAE Transactions*, Vol. 70, 1962, pp. 309-332.

Vita

William E. Nuckolls, Jr. was born in Farmville, Virginia on December 7, 1966. In 1973 he moved to Blacksburg, Virginia and entered grade school. While attending Blacksburg High School he participated in football and track. After graduating from Blacksburg High School he entered Virginia Tech in the fall of 1985. As an undergraduate he was active in the Society of Automotive Engineers Mini-Formula race car design competition. In December 1989 he graduated *summa cum laude* in Mechanical Engineering and immediately began working on a Master of Science degree in January of 1990 at Virginia Tech. As a graduate research assistant he conducted work on the development of a cryogenic turbofan engine simulator and research to reduce fan noise from a supersonic inlet.

After completing his degree, he plans to work for Analytical Services and Material, Inc., as a contractor supporting NASA Langley. He will be working for the Applied Acoustic Branch, developing methods to reduce noise from the next generation of commercial aircraft engines.